



HAL
open science

Catalytic role of solid acid catalysts in glycerol acetylation for the production of bio-additives: a review

Pei San Kong, Mohamed Kheireddine Aroua, Wan Mohd Ashri Wan Daud,
Hwei Voon Lee, Patrick Cognet, Yolande Peres-Lucchese

► To cite this version:

Pei San Kong, Mohamed Kheireddine Aroua, Wan Mohd Ashri Wan Daud, Hwei Voon Lee, Patrick Cognet, et al.. Catalytic role of solid acid catalysts in glycerol acetylation for the production of bio-additives: a review. RSC Advances, 2016, 6 (73), pp.68885-68905. 10.1039/c6ra10686b . hal-01917334

HAL Id: hal-01917334

<https://hal.science/hal-01917334v1>

Submitted on 9 Nov 2018

HAL is a multi-disciplinary open access archive for the deposit and dissemination of scientific research documents, whether they are published or not. The documents may come from teaching and research institutions in France or abroad, or from public or private research centers.

L'archive ouverte pluridisciplinaire **HAL**, est destinée au dépôt et à la diffusion de documents scientifiques de niveau recherche, publiés ou non, émanant des établissements d'enseignement et de recherche français ou étrangers, des laboratoires publics ou privés.



Open Archive Toulouse Archive Ouverte

OATAO is an open access repository that collects the work of Toulouse researchers and makes it freely available over the web where possible

This is an author's version published in: <http://oatao.univ-toulouse.fr/20567>

Official URL:

<https://doi.org/10.1039/c6ra10686b>

To cite this version:

Kong, Pei San and Aroua, Mohamed Kheireddine and Daud, Wan Mohd Ashri Wan and Lee, Hwei Voon and Cognet, Patrick and Peres-Lucchese, Yolande Catalytic role of solid acid catalysts in glycerol acetylation for the production of bio-additives: a review. (2016) RSC Advances, 6 (73). 68885-68905. ISSN 2046-2069

Any correspondence concerning this service should be sent to the repository administrator: tech-oatao@listes-diff.inp-toulouse.fr



CrossMark
click for updates

Cite this: *RSC Adv.*, 2016, 6, 68885

Catalytic role of solid acid catalysts in glycerol acetylation for the production of bio-additives: a review

Pei San Kong,^{ac} Mohamed Kheireddine Aroua,^{*a} Wan Mohd Ashri Wan Daud,^a Hwei Voon Lee,^b Patrick Cognet^c and Yolande Pérès^c

Bio-additives obtained from the acetylation of biodiesel-derived glycerol have been extensively synthesized because of their nature as value-added products and their contribution to environmental sustainability. Glycerol acetylation with acetic acid produces commercially important fuel additives. Considering that the recovery of individual monoacetin, diacetin (DA), and triacetin (TA) is complicated, many endeavours have enhanced the selectivity and total conversion of glycerol using acetic acid during catalytic acetylation. In this work, we extensively review the catalytic activity of different heterogeneous acid catalysts and their important roles in glycerol acetylation and product selectivity. In addition, the most influential operating conditions to attain high yields of combined DA and TA are achieved by closely examining the process. This review also highlights the prospective market, research gaps, and future direction of catalytic glycerol acetylation.

Received 25th April 2016
Accepted 23rd June 2016

DOI: 10.1039/c6ra10686b

www.rsc.org/advances

1. Introduction

Catalytic acetylation of glycerol using acetylating agents, such as acetic acid and acetic anhydride, has been extensively

investigated recently, which is driven by the intention to search for new economic applications of glycerol. Acetic acid is normally used as an acetylating agent in producing biofuel additives *via* acetylation of glycerol; the use of acetic acid is attributed to its lower price (0.5 USD per kg) compared with that of acetic anhydride (about 0.98 USD per kg).¹ S. Sandesh *et al.* reported that the acetylation of glycerol with acetic anhydride required a lower temperature (30 °C) than glycerol acetylation with acetic acid (85 °C).² Despite the fact that glycerol acetylation with acetic anhydride can be conducted at room temperature with low energy utilization, the high potential of

^aDepartment of Chemical Engineering, Faculty of Engineering, University of Malaya, 50603 Kuala Lumpur, Malaysia. E-mail: mk_aroua@um.edu.my; Fax: +60 379675319; Tel: +60 379674615

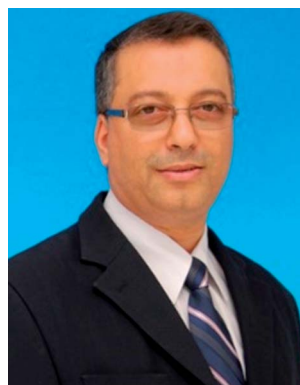
^bNanotechnology and Catalysis Research Centre (NANOCAT), University of Malaya, Level 3, IPS Building, 50603 Kuala Lumpur, Malaysia

^cLaboratoire de Génie Chimique (Labège), BP84234 Campus INP-ENSIACET, 4 allée Emile Monso, 31432 Toulouse Cedex 4, France



Pei San Kong is a joint-PhD candidate of University of Malaya (Malaysia) and INP-ENSIACET, University of Toulouse (France). She holds a bachelor degree in Chemical Engineering and a Master of Engineering Science. She previously worked as an R&D engineer in a Malaysia oleochemical industry and mainly involved in catalysis, process and technology development. Her research inter-

ests include catalysis (heterogeneous/homogeneous acid catalysts), Process engineering (reaction engineering, microwave processing), Energy & Fuels (biodiesel, biolubricant, biofuels) and oleochemical product developments (polyol esters, glycerol derivatives).



Dr Mohamed Kheireddine Aroua is a senior Professor at the Department of Chemical Engineering and the Deputy Dean at the Institute of Graduate Studies, University of Malaya, Malaysia. He is also heading the Center for Separation Science and Technology (CSST). His research interests include CO₂ capture, membrane processes, electrochemical processes using activated carbon, biodiesel

production and conversion of bioglycerol to value added chemicals. He published more than 130 papers in ISI ranked journals with more than 3500 citations. His h-index is 30.

explosion for acetic anhydride is not suitable for manufacturing especially for large-scale production (as above 49 °C explosive vapour/air mixtures may be formed).

On the contrary, the sudden decline in crude oil prices has significantly reduced the prices of biodiesel during the second half of 2014. Fig. 1(a) shows the biodiesel prices declined strongly from 112 USD per hL (2013) to less than 80 USD per hL (2014); the ten year forecast for biodiesel prices are expected to recover in nominal terms close to those in 2014 level (prices vary from 85–90 USD per hL). Fig. 1(b) indicates that the global biodiesel production is expected to reach almost 39 billion liters by 2024; moreover, the projected production volume of biodiesel is stable and is mostly policy driven.³ Nevertheless, conversion of biodiesel-derived glycerol into value-added products is necessary to support long-term growth of the oleochemical market. The price reported for 80% pure crude glycerol is \$0.24 kg⁻¹ and that for United States Pharmacopeia (USP)-grade glycerol is \$0.9 kg⁻¹ in mid-2014.⁴

Various studies on transforming glycerol into different value-added derivatives, such as propylene glycerol, polyglycerols,

succinic acid, gaseous hydrogen, glycerol carbonate, acrolein, fuel additives, ethanol, glycerol esters, and lubricant additive, were conducted.^{5–12} This review aims to study the role of heterogeneous acid catalysts in glycerol acetylation using acetic acid given that the low selectivity of the desired products (diacetin (DA) and triacetin (TA)) remains the greatest challenge in catalytic acetylation. In addition, recovery of key derivatives is a very complicated work because the mono-, di-, and tri-substituted derivatives that constitute a mixture exhibit indistinguishable boiling points.¹ This review then focuses on the important features of solid acid catalysts and on the influence of operating parameters in enhancing the product selectivity of glycerol acetylation. To our best knowledge, this work is the first critical review focusing on the important role of acid heterogeneous catalysts in producing DA and TA as bio-additives.

2. Glycerol derived bio-additives

Glycerol-based additives is suitable for efficient engine performance and is environment friendly.¹³ Table 1 shows four



Dr Wan Mohd Ashri Wan Daud is a Professor at the department of Chemical Engineering University Malaya since 2008. His research interests include activated carbon, pyrolysis process, second generation biodiesel and hydrogen production. He has published more than 160 ISI papers that have garnered more than 3000 citations. His h-index is 27.



Dr Patrick Cognet received his Chemical Engineering Diploma from ENSIC (Ecole Nationale Supérieure des Industries Chimiques de Nancy) and PhD (Electrochemical Engineering) at Chemical Engineering Laboratory, Toulouse. He joins ENSIA-CET (University of Toulouse) as Assistant Professor in 1994 and is a Professor since 2010. His work is focused on Green Process Engineering, more precisely on

reactor design, activation techniques (ultrasound, electrochemistry), intensification and processes involving new media. He created the Green Process Engineering Congress (GPE) in 2007.



Dr Hwei Voon Lee is a senior lecturer at Nanotechnology and Catalysis Research Center (NANOCAT), University of Malaya, Malaysia. She received her PhD in Catalysis (2013) and BSc (Hons) in Industrial Chemistry (2008) from Universiti Putra Malaysia. Her major research interests are Energy & Fuels (biodiesel, renewable diesel, biofuels); Biomass Conversion Technology (catalytic conversion of biomass); Oleochemical Technology (methyl ester, polyol ester), Catalysis (heterogeneous catalyst, mixed metal oxides, acid–base catalyst) and Nano-Materials (biomass derived nanocrystalline cellulose and application).



Dr Yolande Pérès received her PhD in coordination chemistry in 1985 from the University Paul Sabatier (Toulouse, France). She joined the research group of Professor Hoberg at the Max-Planck-Institut für Kohlenforschung (Mülheim an der Ruhr, Germany) as a postdoctoral fellow in 1985. Her research is focused on the transformation of CO₂ and olefins to carboxylic acids catalyzed by transition

metal complexes. After one year in industry, she obtained a position as assistant professor at ENSIACET (University of Toulouse). At present she carries out her research at the Chemical Engineering Laboratory on the topics of catalytic and phytoextraction process.

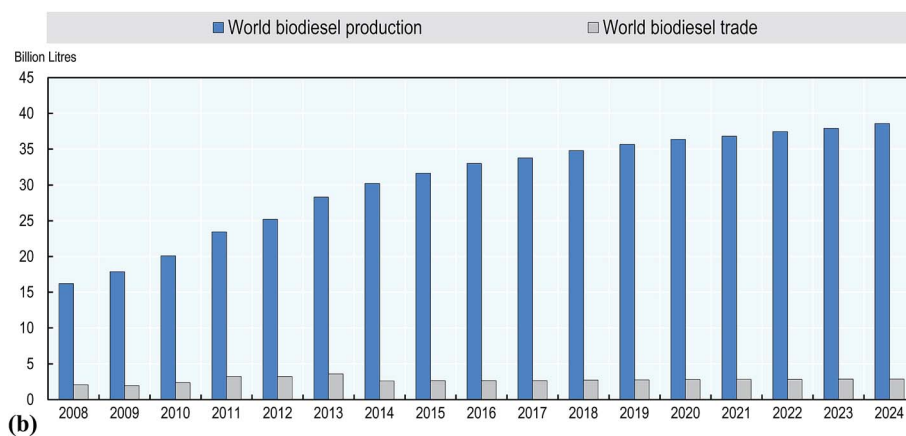
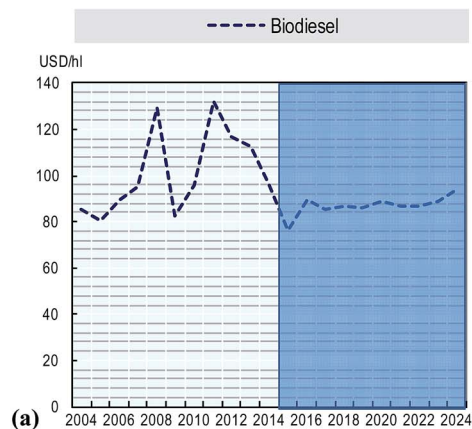


Fig. 1 (a) Evolution of biodiesel world prices. (b) Development of the world biodiesel market (OECD 2015 market report).

important glycerol-derived bio-additives formed by different reactants *via* esterification or acetylation routes. Monoacetin (MA), DA, and TA are produced *via* glycerol acetylation using acetic acid. The specific industrial applications of MA, DA, and TA are summarized. Given that MA is water soluble, DA and TA are the preferred components for bio-additives. MA is proven to be completely soluble in water. By contrast, TA is completely

soluble in ethyl acetate.¹⁴ DA and TA are utilized as fuel bio-additives because they effectively improve cold and viscosity properties, they enhance octane rating, and they can reduce fuel cloud point. Furthermore, TA and DA are alternative for tertiary alkyl ether that causes greenhouse gas emissions.

Glycerol tertiary butyl ether (GTBE) is another potential bio-additive and can be produced *via* glycerol etherification using

Table 1 General product applications of glycerol derived bio-additives

Bio-additives	Starting materials	Product applications	Ref.
(i) MA	Acetic acid; glycerol	<ul style="list-style-type: none"> • Excellent solvency • Plasticizer for cellulose acetate, nitrocellulose, ethyl cellulose and vinylidene polymers 	22 and 23
(ii) DA		<ul style="list-style-type: none"> • Plasticizer for cellulosic polymers and cigarette filter • Raw material for the production of biodegradable polyesters 	13 and 24
(iii) TA		<ul style="list-style-type: none"> • As an antiknock additive for gasoline • Improve cold flow and viscosity properties of biodiesel 	25
(i) GTBE, GDBE	Isobutylene (gas phase); glycerol or <i>tert</i> -butyl alcohol (liquid phase); glycerol	<ul style="list-style-type: none"> • Used in diesel and biodiesel reformulation • Oxygenated additives for diesel fuel • Decreasing cloud point of biodiesel fuel • To reduce fumes, particulate matters, carbon oxides and carbonyl compounds in exhausts 	16 and 17
(i) Di-, tri-GEE	Ethanol; glycerol	(i) Used for fuel formulation	18
(ii) Mono-GEE		(ii) Important intermediate for various chemicals	
Polyglycerols	Glycerol	Excellent lubricity and used as additive in lubricant	20 and 21

gas-phase isobutylene or *via* glycerol etherification using *tert*-butyl alcohol (TBA). The operation cost for gas-phase isobutylene is higher than that for liquid TBA.¹⁵ Isobutylene is obtained from refineries and thus requires additional purification steps to separate isobutylene from C4 mixtures through sulfuric acid extraction or molecular sieve separation. On the contrary, TBA is a biomass-derived compound and is easier to handle during manufacture. Thus, high fraction of glycerol di-*tert* butyl ether (GDBE) is a reliable oxygenated additive for diesel and biodiesel fuels.^{16,17} In addition, a fuel with 10–25 v/v% of oxygenate reduces particulate emission.¹³ Similar to DA and TA, GDBE and GTBE are desired components over glycerol mono-*tert* butyl ether (GMBE) given the low solubility of GMBE in diesel.

Exploitation of sugar-fermented bioethanol for glycerol ethyl ether (GEE) synthesis facilitates production of a completely biomass-derived product.¹⁸ Bioethanol is formerly used as bio-fuel in gasoline engines. However, di- and tri-GEE derivatives are more suitable for diesel and biodiesel formulation because they are water insoluble. Moreover, mono-GEE (dioxolane), a water-soluble secondary compound, is an important intermediate in producing various chemicals.¹⁹ Oligomer diglycerols are synthesized from single-molecule glycerol *via* etherification. Polyglycerols, such as diglycerols, are also widely applied in the pharmaceutical, microbiology, food, and automotive industries,²⁰ as well as used as additives in lubricants.²¹

3. Mechanism acetylation of glycerol

Fig. 2 illustrates the reaction mechanism in MA, DA, and TA production. MA is first produced *via* glycerol acetylation using acetic acid. DA is then synthesized by reacting MA with acetic acid followed by reacting DA with acetic acid to produce TA. Water is produced as by-product during glycerol acetylation.

3.1 Market and demand

China market analysis report revealed that the price of TA remains rigid despite the speculated weakening of the market of TA.²⁶ Fig. 3 demonstrates TA constitutes 10% of the worldwide glycerol market among other uses, which is redrawn on the basis of a previous study.^{27,28} The current global demand for TA is approximately 110 000 T per annum, whereas 35% of demand comes from China. The TA production capacity of China is approximately 55 000 T per annum, 38 500 T of which is intended for domestic consumption and 16 500 T is exported. The price of TA ranges from RM4273–5560 per ton (equivalent to 1097–1428 USD per ton). In addition, the demand for TA is recently growing by 5–10% yearly. The demand for TA is expected to remain strong.²⁹ Dr Kongkrapan Intarajang, Group Chief Executive Officer of Emery Oleochemicals, mentioned in 2012 that the increase in demand for plastic has led to a steady annual growth of 4–5% in plastic additive consumption worldwide.³⁰

3.2 Conventional TA production method

The main manufacturers of TA include Croda, BASF (Cognis), Daicel, Lanxess, ReactChem, Yixing Yongjia Chemical,

Yunnan Huanteng, Klkoleo, and numerous manufacturers from China. The conventional TA manufacturing process involves two steps.²³ Fig. 4 shows the diagram of the conventional TA production. First, glycerol is esterified using acetic acid in the absence of catalyst, where conversion into MA occurs. Water is formed and is removed using an azeotropic distillation system. Second, the produced MAs are further esterified using acetic anhydride under exothermic conditions; TA and acetic acid are formed in this step. Acetic acid is simultaneously recycled as reactant into the first reactor.³¹ Table 2 shows the product specification of food-grade TA.

4. Mechanism of Brønsted and Lewis acid-catalyzed esterification

4.1 General mechanism of glycerol acetylation

Glycerol esterification using acetic anhydride or acetic acid to produce MA, DA, and TA can be extensively explained in the presence of three hydroxyl groups (–OH) that are attached to the glycerol backbone. Acetic acid will selectively attach to any –OH of glycerol or any –OH from partially reacted glycerides; this phenomenon is related to the steric hindrance effect. Thus, the produced MA and DA normally present isomer forms depending on the position of acetylation in the glycerol molecule (Fig. 2).¹³

Among the obtained products, DA and TA are the most interesting products that can be applied as fuel additive. MA is an unfavorable product owing to its relatively high solubility in water. However, direct transformation of the highly selective DA and TA is impossible as the reaction involves a series of consecutive esterification steps, forming various intermediates (glycerides); moreover, each step is driven by chemical equilibrium because of the formation of water as by-product.³³ The selectivity of MA, DA, and TA also depends mostly on the catalyst features (surface acidity, pore structure, and catalyst stability)³⁴ and esterification parameters (glycerol to acetic acid molar ratio, temperature, catalyst amount, and reaction time).³⁵ Furthermore, the acid-catalyzed glycerol acetylation involves two plausible reaction mechanisms based on the types of acid catalyst used: (i) Brønsted acid-catalyzed esterification and (ii) Lewis acid-catalyzed esterification.

4.2 Brønsted acid-catalyzed esterification

The Brønsted acid-catalyzed esterification is also named as Fischer esterification. Fig. 5 shows a conventional reaction mechanism of the esterification reaction. This reaction mechanism involves addition of nucleophile (the glycerol) into acetic acid followed by an elimination step, as follows:³⁶

(i) The acetic acid is initially protonated by the Brønsted-type acid catalyst.

(ii) In the second step, the oxygen atom (two lone pairs) from the –OH of glycerol acts as a nucleophile and attaches to the sp² carbon, leading to the loss of proton from the –OH.

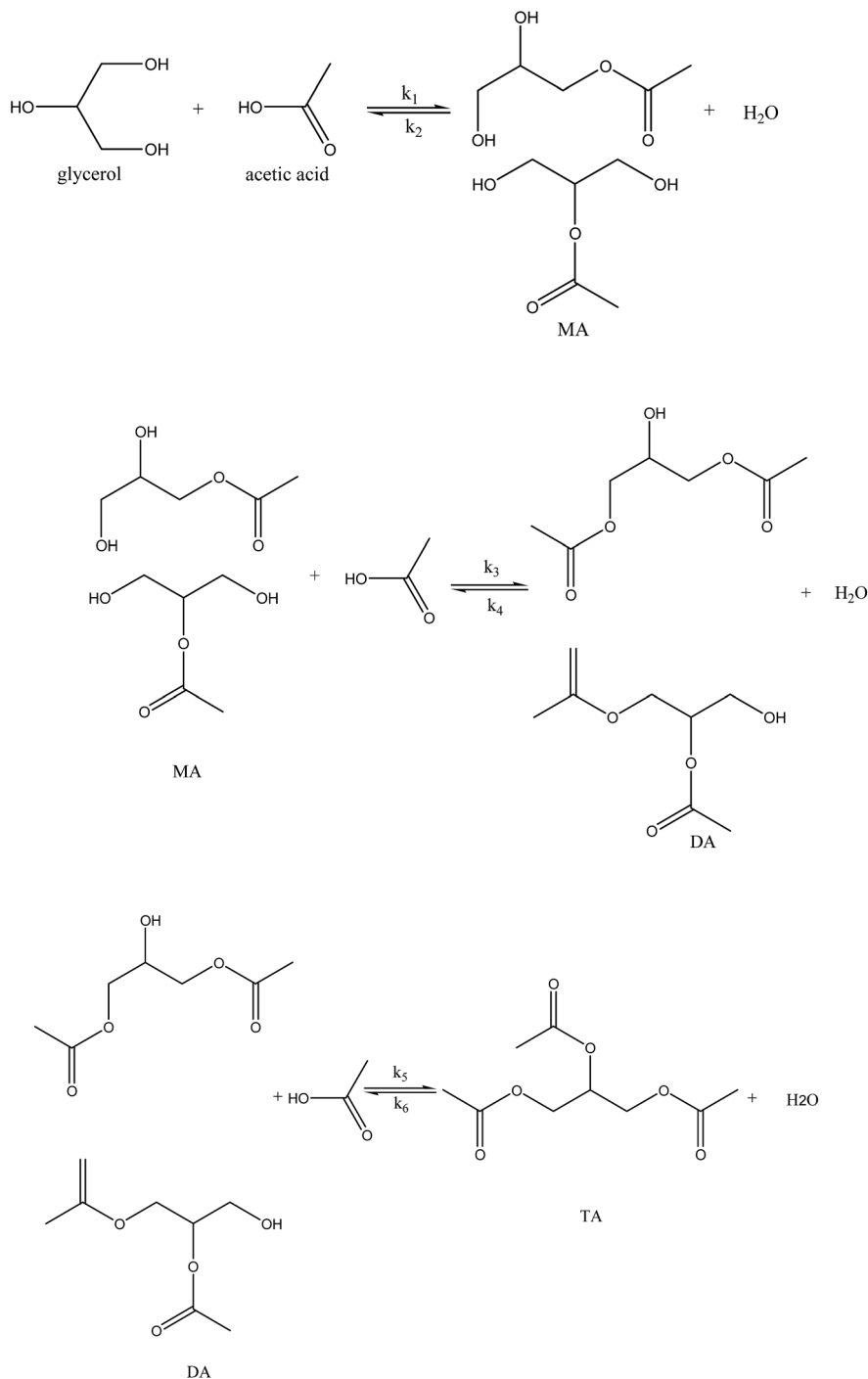


Fig. 2 Reaction mechanism of glycerol acetylation synthesis into MA, DA and TA.

(iii) A series of fast equilibrium proton exchanges occurs in either of the $-\text{OH}$ of acetic acid. In this step, a new ester bond forms between the carboxyl group carbon and the oxygen in glycerol.

(iv) Water is then eliminated in either site.

(v) In the final step, the excess proton leaves, regenerating a Brønsted acid catalyst.

(vi) This process continues until all three strands of the glycerol backbone are converted into esters.

4.3 Lewis acid-catalyzed esterification

Theoretically, Lewis acid-based esterification involves a reaction mechanism similar to that in Brønsted acid-based reaction. In addition, Lewis acid-based esterification involves the attack of glycerol in a nucleophilic addition reaction. A slight difference between these two processes is that the Brønsted-catalyzed reaction uses a proton generated from the acid catalyst. By contrast, the Lewis-based reaction involves a metal cation (Mn^+)

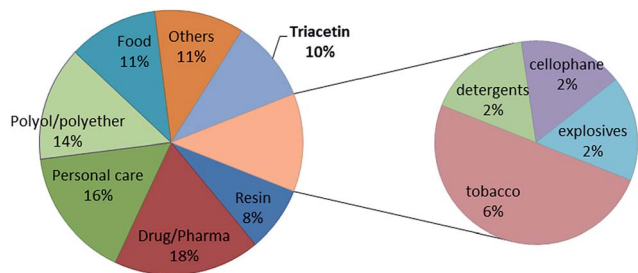


Fig. 3 Distribution of TA in the worldwide glycerol market.

as an electrophile to facilitate the interaction between the carbonyl oxygen from acetic acid and the Lewis acidic site (L^+) of the catalyst to form carbocation. The nucleophile from glycerol attacks the carbon cation and produces tetrahedral intermediates (Fig. 6). During esterification, the tetrahedral intermediate eliminates water molecule to form an ester product.³⁷

5. Heterogeneous acid catalysts for glycerol acetylation

Solid acid catalysts play a crucial role in esterification reaction during ester production. In particular, solid acids have largely replaced the traditional homogeneous acid catalyst because of environmental, technological, and economic reasons. A variety of solid acid catalysts have been studied for glycerol acetylation. Their catalytic efficiency are also categorized into different groups (Table 3).³⁸ The key role of solid acid catalyst in high rate of glycerol conversion and selective formation of DA and TA products include: (i) acidity of catalyst (especially the Brønsted acid sites), (ii) texture, and (iii) surface morphology.

Although many studies have demonstrated the high reactivity of glycerol acetylation, most catalysts exhibit low thermal stability and unsatisfactory selectivity to DA and TA production.³⁹ Furthermore, the hydrophilic character of catalyst surface is a challenge in active site deactivation resulting from the inevitable water formation during esterification, leading to leaching of active components into the reaction medium. The water-tolerant property of solid acid catalyst exhibiting a hydrophobic-enhanced surface is thus necessary to excellently

Table 2 Product specification of TA³²

Property (unit)	Specification
Appearance	Clear liquid free from suspended matter
Odour	Essentially odourless
Purity (%)	>99.5
Colour (Hazen)	<15
Acidity (%)	<0.005
Moisture	<0.05
Arsenic (mg kg^{-1})	<3
Heavy metals (mg kg^{-1})	<5
Viscosity (cP)	21–30
Density 25 °C	1.154–1.158
Refractive index	1.429–1.431

perform glycerol acetylation. Another reason of catalyst deactivation is the partial blockage of the catalyst's active sites by the reaction medium, such as glycerol and/or partial glycerides within the pore structure of catalysts, thereby reducing the number of acid sites for continuous esterification until the desirable end-products are achieved.⁴⁰

5.1 Ion exchange catalyst

Rezayat *et al.* synthesized MA and TA under supercritical carbon dioxide (CO_2) conditions by using the commercially available Amberlyst 15 catalyst.⁴¹ The results showed that the use of catalyst under supercritical CO_2 , as well as the molar ratio of the reactants, determine the yield and selectivity of the product. A 100% selectivity of TA was obtained using the parameters such as 200 bar, 110 °C, and an acetic acid to glycerol molar ratio of 24 for a 2 hour reaction time. However, the selectivity of TA decreased at a reaction time of more than 2 h. The Lewis acidity of CO_2 also influences the reaction.

Dosuna recently investigated glycerol acetylation by using five different ion exchange resins: Amberlyst 15, Amberlyst 36, Dowex 50Wx2, Dowex 50Wx4, and Dowex 50Wx8.⁴² Amberlyst 36 and Dowex 50Wx2 were both outperformed by the other catalysts when reaction was performed at 105 °C, at a glycerol to acetic acid molar ratio of 8 : 1, under atmospheric pressure, at a 6.25 g of dry catalyst/L of glycerol ratio,

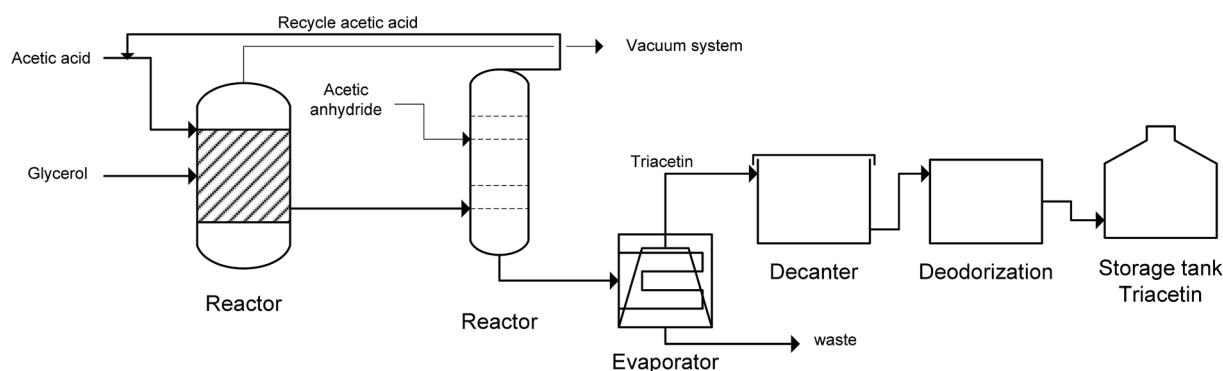


Fig. 4 Process flow diagram of conventional TA production.

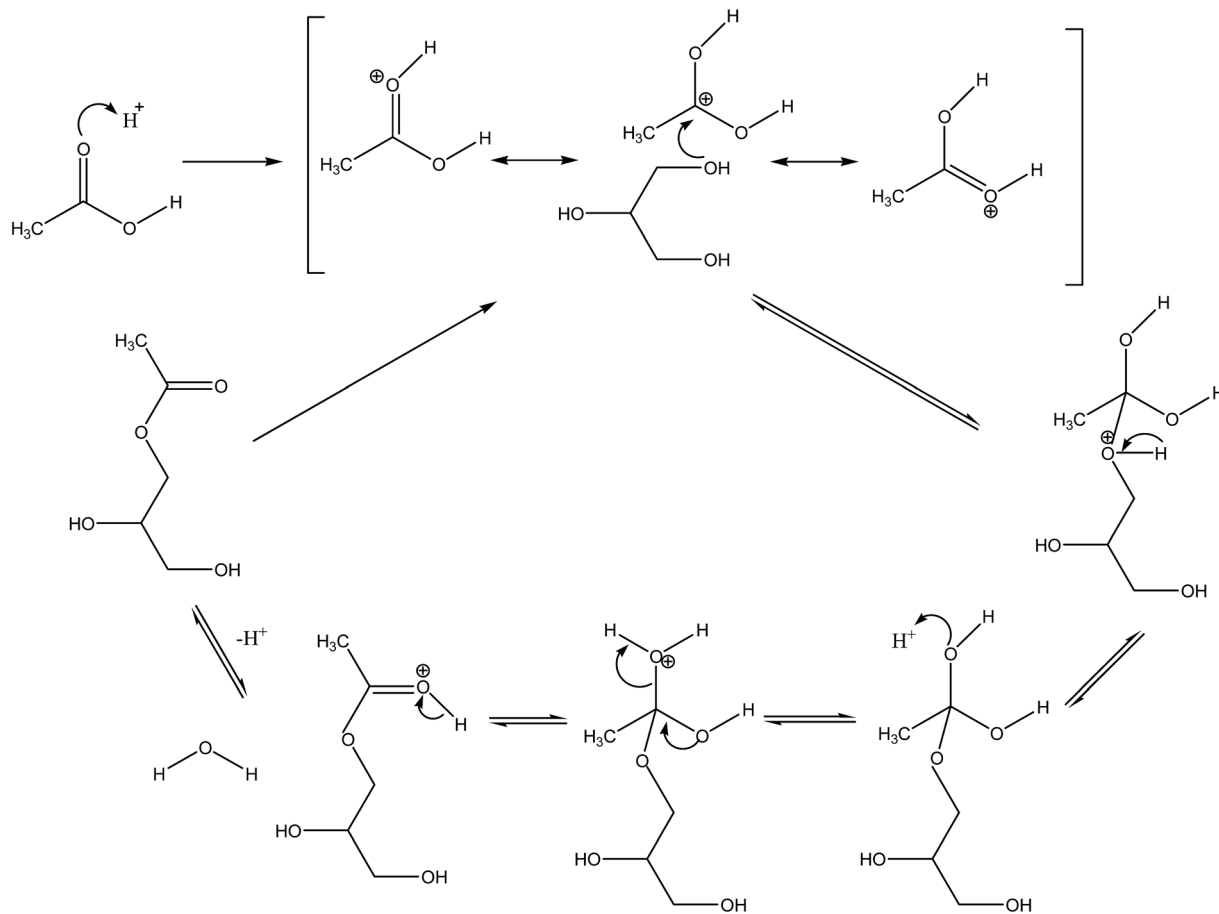


Fig. 5 Brønsted-acid reaction mechanism.

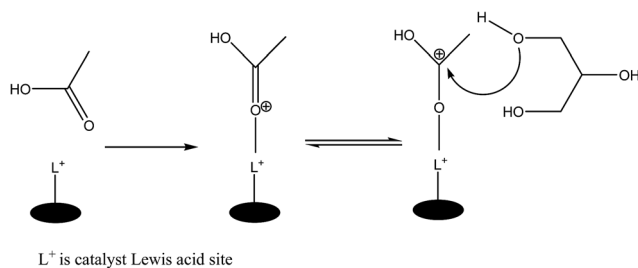


Fig. 6 Lewis acid reaction mechanism.

and at a 10 hour reaction time. Unlike the previous studies, this work was aimed to produce high selectivity of MA. The use of Amberlyst 36 resulted in 70.3% MA selectivity, whereas Dowex 50Wx2 produced 80.8% selectivity of MA with excess of glycerol. Our result showed that high selectivity toward formation of small MA molecule was caused by cross-linkage of the catalyst.

Zhou demonstrated that the Amberlyst 15-catalyzed glycerol acetylation produced high selectivity of DA and TA.³⁵ High amount of acid sites and sufficient pore spaces are the vital factors in formation of large molecular DA and TA derivatives. However, Amberlyst 15 exhibits weak acid strength, leading to low glycerol conversion. In addition, the leaching of catalyst

Amberlyst 15, resulting from the loss of functional groups through hydrolysis at operating temperatures above the polymer thermal stability limit ($>120\text{ }^\circ\text{C}$) should be considered in acetylation process.¹² As A. Ignatyev Igor *et al.*⁴³ observed the phenomenon of protons leaching from the Amberlyst 15 in the synthesis of glucose esters from cellulose *via* hydrolysis–acetylation steps. Therefore, Wang developed an improved swelling-changeable polymer catalyst by using sodium 5,5′-sulfonylbis(2-chlorobenzenesulfonate) and bis(4-chlorophenyl)sulfone to increase selectivity and conversion of glycerol acetylation.⁴⁴ The improved polymer-based acid (PES) catalyst exhibits stronger acid strength (two times stronger than Amberlyst 15) and better swelling property, resulting in glycerol conversion of 98.4% with 94.9% total selectivity of DA and TA. The high acid strength of PES catalyst is attributed to its electron-withdrawing $-\text{SO}_2^-$ group.

5.2 Zeolite-based acid catalyst

Zeolites are microporous crystalline solids that offer wide application in oil refining industry, petrochemistry, and fine chemical production. Zeolites are generally categorized as aluminosilicate minerals, which are applied as catalyst support for active species owing to their unique pore system, high surface area, and high stability. Different zeolite systems,

Table 3 Different groups of solid acid catalysts for glycerol acetylation

Solid acid catalysts	Properties
Ion exchange resin	<ul style="list-style-type: none"> • Ion exchange resins are synthesized from polymers that are capable of exchanging particular ions. The drawback of the ion exchange resin catalyst is its low temperature stability
Zeolites	<ul style="list-style-type: none"> • Crystalline solids composed of silicon and aluminum oxides arranged in a three-dimensional network of uniformly shaped micropores (<2 nm) of tuneable topology and composition • Brønsted acid sites in zeolites are commonly generated when protons balance the negatively charged framework induced by the presence of tetrahedrally coordinated aluminum (Al) atoms
Heteropolyacids Metal oxides	<ul style="list-style-type: none"> • A class of metal salts wherein the oxo-anions are balanced by a wide range of cations with varying acid strength • The Brønsted acid sites in metal oxides originate from highly polarized hydroxyl groups, acting as proton donors • The Lewis acid sites generated from coordinatively unsaturated cationic sites, which leave M^+ exposed to interact with guest molecules as an acceptor of pairs of electrons
Mesoporous silica	<ul style="list-style-type: none"> • Mesoporous silica is a mesoporous form of silicate that consists of unique features: high surface area, chemical, thermal, and mechanical stability, highly uniform pore distribution and tunable pore size, high adsorption capacity, and an ordered porous network • This material is potentially used as solid supported catalyst due to its recyclability, enhanced catalytic reactivity, and selectivity
Carbon	<ul style="list-style-type: none"> • Porous carbon is an attractive catalytic material as it can be prepared from various low-cost waste carbon materials • This material consist of suitable characteristics that can be used as a catalyst support, such as heat resistance, stability in both acidic and basic media, the possibility of easy recovery of precious metals supported on it and the possibility of tailoring both its textural and surface chemical properties

including ZSM-5, zeolite-beta, and USY, can be applied as potential catalysts in glycerol esterification/acetylation.⁴⁵

The catalytic esterification reaction over zeolite-based catalysts depends on their different crystal structure, Si/Al ratio, and proton exchange level; these properties allows the catalytic properties, such as pore size, hydrophobicity/hydrophilicity, Brønsted/Lewis acidity, and acid strength distribution, to be designed. For esterification, surface acidity is the most vital characteristic in designing a zeolite-based catalyst. The acidity of zeolite can be tuned by altering their chemical composition (Si/Al ratio) and ion-exchange abilities. Theoretically, protonic zeolite consisting of bridging -OH groups (Al-(OH)-Si) is an active acid site that favors Brønsted acid-catalyzed esterification reactions (Fig. 7 (ref. 46)). Zeolites exhibiting low Al framework are the most hydrophobic types. In addition, acidity measurements of zeolites normally comprise both Brønsted and Lewis acid sites, acid strength distribution, and precise location of the acid sites.⁴⁷

Gonçalves *et al.* investigated the production of MA, DA, and TA during glycerol acetylation using acetic acid and catalyzed by the zeolites HZSM-5 and HUSY. The reactivity of the zeolite catalyst was also compared with that of the traditional acid

catalysts, such as Amberlyst-15 acid resin, clay K-10 montmorillonite, and niobic acid. Although the zeolites HZSM-5 and HUSY exhibit high surface area (374 and 566 $m^2 g^{-1}$, respectively), their acidity were lower than that of Amberlyst-15 (HZSM-5 zeolite = 1.2 $mmol g^{-1}$; HUSY zeolite = 1.9 $mmol g^{-1}$; and Amberlyst-15 = 4.2 $mmol g^{-1}$). Given that the esterification rate mostly depends on the catalyst's acidity, the decreasing order of acetylation is as follows: Amberlyst-15 > K-10 clay > niobic acid \sim HZSM-5 > HUSY. The poor performance of zeolites is possibly related to difficulty of diffusion of acetylated esters within the catalyst's cavities. This phenomenon resulted in low selectivity of DA and TA as both molecules are space demanding and their formation and diffusion within the zeolite pores are difficult.⁴⁸

Ferreira *et al.* attempted to improve the catalytic activity of esterification by enhancing the acidity of zeolite-based acid catalysts. Dodeca-molybdophosphoric acid ($H_3PMo_{12}O_{40}$) was encaged in USY zeolite for glycerol acetylation. $H_3PMo_{12}O_{40}$ is known as heteropolyacid with strong Brønsted acidity and is widely applied as acid catalyst in esterification. Nonetheless, $H_3PMo_{12}O_{40}$ exhibits low specific surface area (1–10 $m^2 g^{-1}$) and

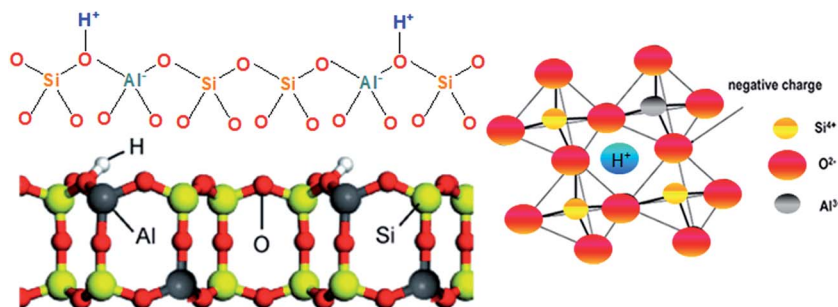


Fig. 7 Brønsted acidity of zeolite in esterification reaction.

low thermal stability. Therefore, encapsulation of $\text{H}_3\text{PMo}_{12}\text{O}_{40}$ in acid supercages of NaUSY support increased the number of accessible acid sites at a surface area of $713 \text{ m}^2 \text{ g}^{-1}$. Moreover, the 1.9 wt% dosing of PMo zeolite catalyst demonstrated the highest catalytic activity, with 59% selectivity of DA and 68% total glycerol conversion.²⁴

5.3 Heteropolyacids (HPAs)-based acid catalyst

HPAs, such as silicotungstic acid (HSiW), phosphotungstic acid (HPW), and phosphomolybdic acid (HPMo), are typical Brønsted acids containing a superacid region that displays outstanding catalytic esterification activity both in homogeneous and heterogeneous phases. HPAs are complex proton acids that incorporate the Keggin-type polyoxometalate anions (heteropolyanions) containing metal–oxygen octahedra with a formula $\text{XM}_{12}\text{O}_{40}^{x-8}$, where X is the central atom ($\text{Si}^{4+}/\text{P}^{5+}$), x is its oxidation state, and M is the metal ion (Mo^{6+} or W^{6+}).⁴⁹ The acid strength of crystalline HPAs generally decreases in the following order: $\text{PW} > \text{SiW} \geq \text{PMo} > \text{SiMo}$, which is identical to the dissociation constants presented in Table 4. Moreover, HPAs in solution are stronger than the usual mineral acids, such as H_2SO_4 , HCl, and HNO_3 .⁵⁰ However, bulk HPAs exhibit low thermal stability, low surface area ($1\text{--}10 \text{ m}^2 \text{ g}^{-1}$), and are highly soluble in polar media (water, lower alcohols, ketones, ethers, esters, *etc.*), which restricts their application as solid acid catalyst in esterification reaction.

Researchers have improved the thermal stability, surface area, and solubility of HPAs in polar media by exchanging the protons of HPA with metal/alkali metal ions and by supporting bulk HPA with a suitable acidic or neutral carrier (such as SiO_2 , active carbon, acidic ion-exchange resin, or metal oxide). Zhu utilized zirconia as a support material to develop HPA-based catalyst.⁵¹ HPAs display excellent catalytic performance over a wide variety of acid-catalyzed reactions owing to their low corrosiveness, well-built structure, as well as adjustable acidity. Nevertheless, HSiW is deemed more active than the other available HPAs, such as HPW and HPMo. HSiW consists of four Keggin protons and advanced Brønsted acid sites, as well as exhibits stronger hydrothermal stability, making HSiW considerably superior over the two other HPAs. Therefore, the activity of HSiW supported with ZrO_2 ($\text{H}_4\text{SiW}_{12}\text{O}_{40}/\text{ZrO}_2$) in glycerol acetylation at $120 \text{ }^\circ\text{C}$, 0.8 wt% of catalyst, 1 : 10 molar ratio of glycerol : acetic acid for 4 h reaction time, was investigated. Three vital findings were revealed: (i) $\text{H}_4\text{SiW}_{12}\text{O}_{40}/\text{ZrO}_2$ is

a predominant glycerol esterification catalyst as it can be reused up to four continuous runs without showing any deactivation; (ii) $\text{H}_4\text{SiW}_{12}\text{O}_{40}/\text{ZrO}_2$ can be directly used to catalyze crude glycerol material; and (iii) a 93.6% combined selectivity of DA and TA was achieved.

Glycerol acetylation over 12-tungstophosphoric acid (TPA) supported on Cs-containing zirconia ($\text{TPA}/\text{Cs}_x\text{-ZrO}_2$) catalyst was investigated to improve the selectivity of MA, DA, and TA formation.⁵² The comparative study of different Cs amount doped on ZrO_2 support was insight studied to evaluate the catalyst activity towards glycerol acetylation. Given that the partial substitution of H^+ by Cs^+ has altered the total number of available surface acid sites, the TPA–Cs catalyst demonstrated better esterification activities than the TPA parent acid during the reaction. In addition, this work revealed that the $\text{TPA}/\text{Cs}_2\text{-ZrO}_2$ catalyst (with Cs amount equal to 2-protons of TPA) demonstrated the highest acidity and catalytic activity compared to zero or excess Cs content of catalysts. By contrast, the zero Cs-content catalyst yielded the lowest conversion, while the catalyst with Cs amount equal to 3-protons of TPA also showed low activity owing to the absence of residual protons. This work concluded that the catalytic activity, acidity and textural properties of the catalyst are varied with the amount of Cs present on support. Where, the presence of exchangeable Cs content has improved the surface acidic sites resulting from the existence of residual protons. Conversion of more than 90% can then be achieved within 2 h. When the reaction time was prolonged to 4 h at $120 \text{ }^\circ\text{C}$, 1.5 acetic acid to glycerol molar ratio, and 0.2 wt% of catalyst concentration, the selectivity towards DA and TA is 55% and 5%, respectively.

Further, S. Sandesh *et al.* reported glycerol acetylation with acetic acid under mild reaction condition in the presence of cesium phosphotungstate catalyst (CsPW).² CsPW catalyst was prepared by precipitation of 0.75 M HPW solution with 0.47 M aqueous cesium carbonate. This study revealed that the conversion and selectivity of DA and TA were greatly influenced by the total acidity of catalyst (1.87 mmol g^{-1}) and Brønsted acidic sites of CsPW catalyst. The comparative characterization results for original HPW and Cs-precipitated CsPW catalyst have confirmed that CsPW catalyst exhibits significant centered cubic assembly and unaltered primary Keggin structure. In addition, CsPW catalyst has the highest Brønsted to Lewis acid ratio compared to Amberlyst 15, sulfated zirconia, H-beta and K-10 catalysts. Apparently the Cs content in CsPW catalyst has altered the textural properties (with $110 \text{ m}^2 \text{ g}^{-1}$ specific surface area), acidity as well as its catalytic activity towards acetylation. The acetylation of glycerol with acetic acid resulted in conversion of more than 98% and total 75% selectivity of DA and TA at 7 wt% of CsPW catalyst, $85 \text{ }^\circ\text{C}$ reaction temperature, 8 : 1 molar ratio of acetic acid to glycerol for 120 min reaction time.

Patel *et al.* recently investigated the use of TPA anchored on two types of support, namely, zirconia and MCM-41, for glycerol acetylation. The use of catalyst support successfully improved the mechanical stability of TPA and enabled catalytic activity modification. These results confirmed that the MCM-41-supported TPA rendered high esterification activity (conversion of 87% and 60% selectivity of DA). By contrast, the ZrO_2 -

Table 4 Dissociation constants of HPAs in acetone at $25 \text{ }^\circ\text{C}$ (ref. 50)

Acids	$\text{p}K_1$	$\text{p}K_2$	$\text{p}K_3$
$\text{H}_3\text{PW}_{12}\text{O}_{40}$	1.6	3.0	4.0
$\text{H}_4\text{PW}_{11}\text{VO}_{40}$	1.8	3.2	4.4
$\text{H}_4\text{SiW}_{12}\text{O}_{40}$	2.0	3.6	5.3
$\text{H}_3\text{PMo}_{12}\text{O}_{40}$	2.0	3.6	5.3
$\text{H}_4\text{SiMo}_{12}\text{O}_{40}$	2.1	3.9	5.9
H_2SO_4	6.6		
HCl	4.3		
HNO_3	9.4		

supported TPA resulted in low conversion (80%) and 36% selectivity of DA. The high-acidity profile and specific hexagonal channels of MCM-41 also facilitated the diffusion of functional glycerol molecule compared with those of ZrO_2 .⁵³

Given that the acidity and esterification activity of HPA-based catalyst is improved by exchanging the protons of HPA with different cations, another group researcher designed a silver-modified HPW catalyst (HPW/Ag), which was prepared through the ion-exchange method. The HPW/Ag catalyst consists of high number of Brønsted acid and Lewis acid sites and exhibits excellent water tolerance, strong stability in polar reaction environment, and a unique Keggin structure (these properties are responsible for the tremendous esterification reaction). The reaction was performed at 120 °C, 10 wt% of catalyst, and 4 : 1 acetic acid to glycerol molar ratio under vigorous mixing at 1200 rpm for 4 h. A total of 96.8% conversion and 90.7% selectivity towards DA and TA was attained. The advantage of the HPW/Ag catalyst is the existence of identical symmetry like parent HPW together with a bonded unit cell in the form of dihydronium ions H_2O_2^+ , where it is formed by protons exchange in the secondary Keggin structure. Neither leaching nor deactivation was detected in five consecutive reaction cycles.⁵⁴

In addition, niobic acid-supported tungstophosphoric acid catalyst (TPA/ Nb_2O_5) for glycerol acetylation was studied.⁵⁵ TPA Keggin ion (25 wt%) was well-dispersed in the niobic acid support (25 wt% TPA/ Nb_2O_5). The catalyst demonstrated high total conversion (90%) and 76% selectivity towards DA and TA at operating parameters of 120 °C, 1 : 5 glycerol to acetic acid molar ratio, and catalyst weight of 200 mg for a 4 hour reaction time. The findings of this work suggested that glycerol acetylation conversion and selectivity depend on catalyst acidity, which is highly related to the content of niobic acid-supported TPA.

5.4 Metal oxide-based acid catalyst

The use of metal oxide-based catalysts for esterification reaction has attracted attention owing to their strong surface acidity and high activity at low operating temperatures. The presence of Lewis acid (cations) and Brønsted acid (OH^- group)/Brønsted base (O^{2-} group) (anions) of metal oxides provided the required catalytic sites for esterification. Fig. 8 illustrates the existence of Lewis and Brønsted sites in the metal oxide catalyst.³⁸ Moreover, functionalization of metal oxide *via* sulphonation (sulfated metal oxides, such as sulfated-zirconia, -tin oxide (SnO_2), -titanium oxide, and -mixed oxides) is a convenient means of enhancing the surface area and acidity of a catalyst.

Malleshham reported that SnO_2 is one of the potential metal oxide solid acid catalysts prepared through the wet impregnation method, where SO_4^{2-} , MoO_3 , and WO_3 were incorporated into the SnO_2 support. Compared when metal oxide is used alone, incorporation of promoters into SnO_2 can enhance the

thermal stability and catalytic performance of SnO_2 . The performance of three catalysts in esterification of acetic acid using glycerol was comparatively investigated. The results showed that all of these catalysts consisted of both Brønsted and Lewis acidic sites. The ascending order of the activities of the catalysts is as follows: $\text{SnO}_2 < \text{WO}_3/\text{SnO}_2 < \text{MoO}_3/\text{SnO}_2 < \text{SO}_4^{2-}/\text{SnO}_2$. The sulfated SnO_2 ($\text{SO}_4^{2-}/\text{SnO}_2$) showed the highest performance mainly because of the presence of large number of acidic sites associated with super acidic sites.⁵⁶

Mixed metal oxide system offers interesting and enhancing properties, especially when each component differs remarkably from each other. Mixed metal oxide catalysts can generally be prepared *via* co-precipitation, impregnation, or sol-gel methods from its bulk oxide or metal salt as precursors.⁵⁷ The binary metal oxide system often establishes new acid sites or modulates the acid properties of the bulk oxides, which are active during esterification.⁵⁸ For instance, sulfated binary oxide solid superacids ($\text{SO}_4^{2-}/\text{TiO}_2\text{-SiO}_2$) synthesized by Yang *et al.* was utilized as catalyst in glycerol esterification using acetic acid under toluene solvent-reaction system.⁵⁹ The $\text{TiO}_2\text{-SiO}_2$ showing the highest catalytic quality was calcined at 450 °C and consists of 13.8 wt% of TiO_2 . Yang reported that the coupling of two oxides ($\text{TiO}_2\text{-SiO}_2$) can generate stronger acid sites and higher acidity compared with bulk metal oxide owing to the larger specific surface area of the coupling. Whereby, the presence of strong acidity of $\text{SO}_4^{2-}/\text{TiO}_2\text{-SiO}_2$ is initiated by an excess of a negative or positive charge in a binary oxide. The TiO_2 content, special surface area and unique structure of modified $\text{SO}_4^{2-}/\text{TiO}_2\text{-SiO}_2$ catalyst resulted in 91.4% conversion.

Reddy *et al.* performed similar glycerol esterification using acetic acid catalyzed by various types of zirconia-based catalysts: ZrO_2 , $\text{TiO}_2\text{-ZrO}_2$, $\text{WO}_3/\text{TiO}_2\text{-ZrO}_2$, and $\text{MoO}_3/\text{TiO}_2\text{-ZrO}_2$. $\text{MoO}_3/\text{TiO}_2\text{-ZrO}_2$ showed the highest conversion among the investigated catalysts. A 100% conversion with 80% selectivity towards TA was achieved at 120 °C, acetic acid to glycerol molar ratio of 6 : 1, and 5 wt% of catalyst concentration for 60 h reaction time.²⁵ The results revealed that the MoO_3 promoted the number of acidic sites of $\text{TiO}_2\text{-ZrO}_2$ support and the strong interaction between the dispersed MoO_3 with support have increased catalytic activity for glycerol acetylation. Despite its high conversion and selectivity, long operation time is required for TA production, which is not cost-effective toward upscaling for industrial uses.

Reddy *et al.* further improved the activity and selectivity of products (DA and TA) by using a modified sulfonated zirconia-based mixed metal oxide; they used a better metal oxide support ($\text{SO}_4^{2-}/\text{CeO}_2\text{-ZrO}_2$) for acetylation. The wet impregnated sulfate ions on $\text{CeO}_2\text{-ZrO}_2$ mixed oxides has increased the initial metal oxide surface area resulting from the formation of porous surface sulfate compounds between the sulfate groups and the supports. The reaction time was successfully shortened to 1 h, and a high glycerol conversion (100%) and 74.2% selectivity towards DA and TA was achieved. Nevertheless, a longer reaction time (40 h) was required for the steric structure of partial glycerides to esterify into 90% highly selective TA.⁶⁰

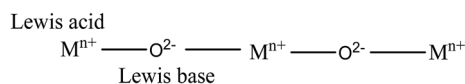


Fig. 8 Lewis and Brønsted site of metal oxide catalyst.

5.5 Mesoporous silica-based catalysts

Mesoporous silica materials, such as MCM-41 and SBA-15, have attracted much attention as a catalyst support in heterogeneous catalysis owing to their high specific surface area ($\geq 1000 \text{ m}^2 \text{ g}^{-1}$), well-ordered mesoporous structure, and large pore sizes ($2 \text{ nm} \leq \text{size} \leq 20 \text{ nm}$).⁶¹ The preparation of sulfonated silica is shown in Fig. 9, as redrawn on the basis of previous study.⁶² Given that they display a high accessibility to large organic molecules, such as fatty acids and esters, the mesoporous silica-based catalysts were chosen as acid catalysts for esterification of glycerol with fatty acids, especially when these catalysts are functionalized with R-SO₃H groups.⁶³ The plausible mechanism of esterification of acetic acid using methanol and catalyzed by acid-functionalized SBA-15 was reported by Miao.⁶⁴ The functionalized SBA-15 obeyed dual-site mechanism (Langmuir-Hinshelwood type), which involved adsorption of both acetic acid and alcohol molecules. This phenomenon demonstrated that the reaction occurred at a high rate. Fig. 10 illustrates the dual-site esterification mechanism catalyzed by functionalized SBA-15, which is modified on the basis of a previous study.⁶⁴

The SBA-15 silica-based catalysts are often modified as novel solid acid catalysts for TA and DA production. SBA-15 possesses unidirectional channels arranged in hexagonal symmetry and interconnected by micropores. The cross-sectional area of this catalyst is speculated to be much larger than that of MCM-41.^{65,66} SBA-15 exhibits a large surface area ($700\text{--}900 \text{ m}^2 \text{ g}^{-1}$), large pore size ($5\text{--}9 \text{ nm}$), and thick walls ($3.5\text{--}5.3 \text{ nm}$).⁶⁷ Gonçalves *et al.* used five different solid acids (Amberlyst-15, K-10 montmorillonite, niobic acid, HZSM-5, and HUSY) to produce DA and TA. Among the tested catalysts, Amberlyst-15 (acidity = 4.2 mmol g^{-1}) was the most active, showing 97% conversion and 67% selectivity of DA and TA, followed by K-10 clay (acidity = 0.5 mmol g^{-1}) with 96% conversion but a lower combined selectivity of DA and TA (54%).⁴⁸ Despite of K-10 clay does not possess high acidity, the predominant of medium-weak

Brønsted acid sites of K-10 clay are mainly responsible for catalytic activity as K-10 clay is type of acetic acid-treated catalyst.^{68,69} As shown by the recent studies, the use of SBA-15 as solid acid catalyst has demonstrated enormous improvement in terms of conversion and selectivity. For instance, a hybrid SBA-15 catalyst functionalized with molybdophosphoric acid (MPA/SBA-15) can achieve 100% glycerol conversion with a corresponding 86% combined selectivity of DA and TA. The thermal decomposition of 15% MPA over SBA-15 support has shown improved catalytic activity in glycerol acetylation using acetic acid.⁷⁰

Trejda *et al.* also modified the SBA-15 catalyst. They modified the mesoporous niobiosilicate (nb-SBA-15) with 3-mercaptopropyl trimethoxysilane (MPTMS) followed by hydrogen peroxide oxidation of the thiol species of the catalyst (denoted as MP-nb-SBA-15 catalyst). The work revealed that, compared with silica material, the presence of niobium in the matrix improved the transformation of thiols into sulphonic species *via* hydrogen peroxide oxidation. The optimum Si/MPTMS ratio is 1 : 1. The elemental analysis of the catalysts revealed that the inclusion of MPTMS into nb-SBA-15 is effective and has reduced the surface area, pore volume, and pore diameter. Thus, the modified catalyst used in this work does not only change the conversion but also strongly affects the selectivity. The dominant product is DA (approximately 50%), and a considerably high selectivity of TA of up to nearly 40% was attained. Nevertheless, weak stability of catalyst was detected during recyclability test.⁷¹

Catalytic esterification of yttrium supported on silicate framework (Y/SBA-3) during glycerol acetylation was also studied. Grafting of yttrium on silicate framework increased the surface area of Y/SBA-3 ($1568 \text{ m}^2 \text{ g}^{-1}$) compared with that of the blank silicate (SBA-3 at $1462 \text{ m}^2 \text{ g}^{-1}$), confirming the inhibitory effect of nano-sized yttrium agglomeration. The Y/SBA-3 used to catalyze glycerol acetylation, resulting in 100% glycerol conversion and 89% combined selectivity of DA and TA. The

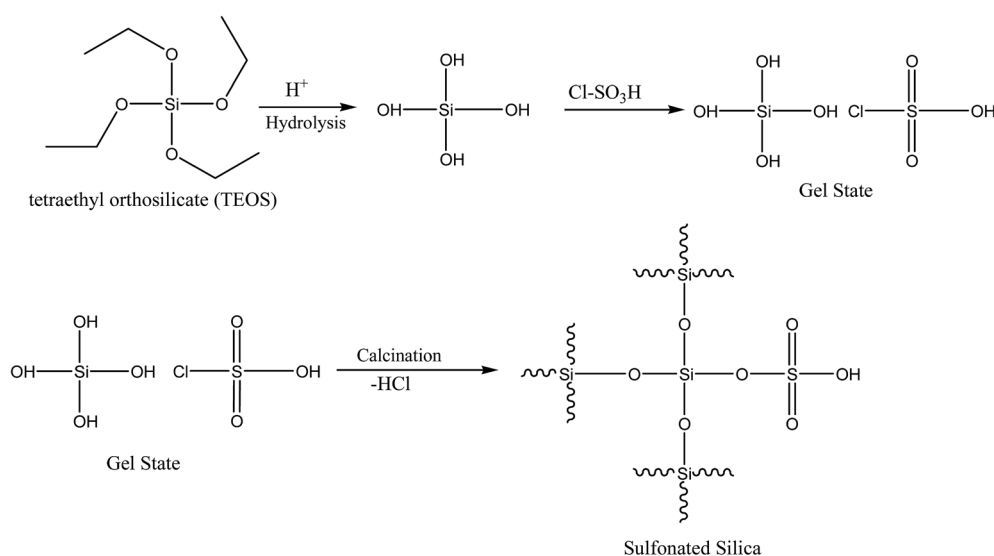


Fig. 9 Preparation of sulfonated silica.

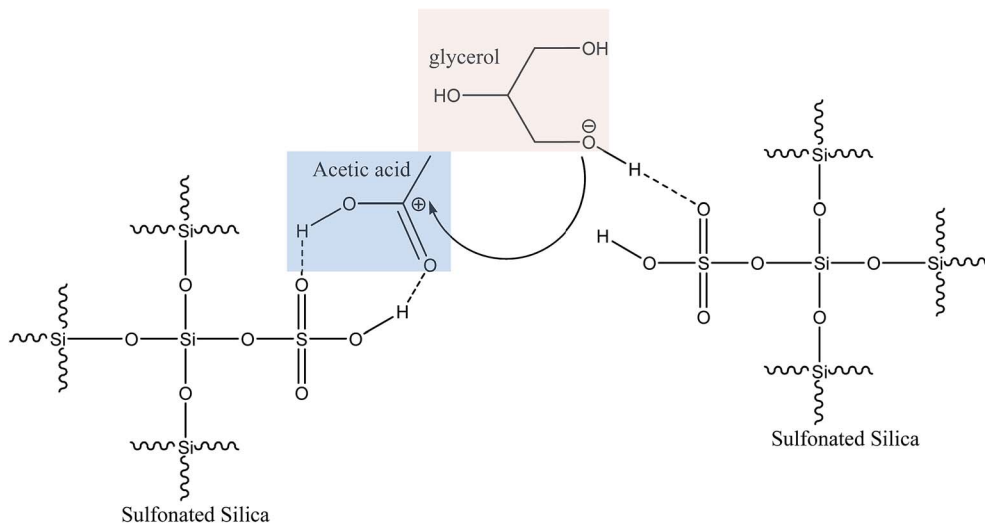


Fig. 10 Dual-site esterification mechanism (Langmuir–Hinshelwood type, L–H) through functionalized SBA-15 catalyst.

catalyst activity was greatly influenced by two factors: (i) acidity of the catalyst and (ii) the combination of high surface area and large pore size, which facilitated the diffusion of bulky glycerol and the final product. This work also compared the catalytic activities of different SBA-15-based catalysts and found that the decreasing order of the catalytic activity is as follows: 3%Y/SBA-3 > SBAH-15 (15) (hybrid SBA-15 functionalized with molybdophosphoric acid) > AC-SA5 (sulfated activated carbon).⁴⁰

Although mesoporous silica has displayed good performance in esterification, Stawicka further improved the mesoporous support by creating more open structures, which improve the performance of the catalyst during esterification using glycerol and acetic acid. Mesostructured cellular foams (MCF) containing acidic sites derived from oxidized MPTMS were developed. Fig. 11 shows the simplified model of the MCF structure. MCF consists of uniform spherical cells approximately 20–40 nm in diameter and possesses surface areas up to approximately 900 m² g⁻¹. The cells are interconnected by uniform windows (7–20 nm in diameter), forming a continuous 3-D pore system. In addition, the walls of the MCFs are formed from silica; the silanols present on the surface can thus be used to modify the material. The presence of niobium (Nb/MCF) and tantalum (Ta/MCF) doped on the MCF also improves the Brønsted acidity of the catalyst. The acidic sites of Nb/MCF and

Ta/MCF catalysts were derived from the oxidized MPTMS and were further enhanced by modification with Nb and Ta. Interestingly, the sulphonic species on silica surfaces showed high stability and strength after being modified by the presence of promoters. Both Nb/MCF and Ta/MCF showed high conversion and selectivity of DA and TA even though the acidity of Ta/MCF (0.57 mequiv. g⁻¹) was higher than that of Nb/MCF (0.32 mequiv. g⁻¹).⁷²

5.6 Mesoporous carbon-based acid catalyst

Mesoporous carbon has been actively studied generally as a catalyst support and/or acid-functionalized carbon for esterification reaction. The presence of surface oxide group in mesoporous carbon enables it to provide anchoring sites for active metals, which can tune the properties of carbon as a catalyst support material. Furthermore, the existence of unique properties, such as high thermal–mechanical stability with low metal leaching, as well as controllable textural and surface chemical properties, makes carbon a suitable catalyst support. Compared with mesoporous silica, mesoporous carbon is more resistant to structural changes caused by hydrolytic effects in aqueous environments. Acid-functionalized carbon, such as sulfonated-carbon *via* sulfonation by concentrated H₂SO₄ (formation of high density sulfonic acid group (–SO₃H)), has been extensively studied in esterification. Fig. 12 shows the preparation of sulfonated carbon.^{73,74}

Sulfonated activated carbon (AC) was investigated in glycerol esterification using acetic acid to produce DA and TA. The porosity of the AC was measured, and the results revealed that 27% of the AC exhibits mesoporous structure. A blank AC normally exhibits large specific surface area of up to 780 m² g⁻¹. This work found that the acid treatment has slightly reduced the surface area of AC to 742 m² g⁻¹. The acid-functionalized AC was prepared through hydrothermal treatment with sulfuric acid at 85 °C for 4 h. Although the sulfonated AC catalyst (AC-SA5) demonstrated good stability during recycling (up to four

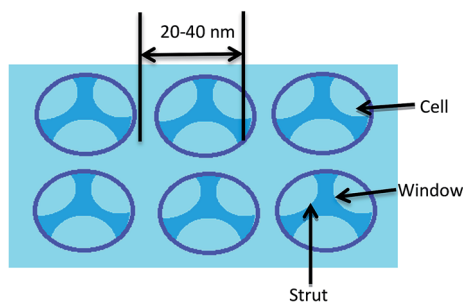


Fig. 11 Simplified model of MCF structure.

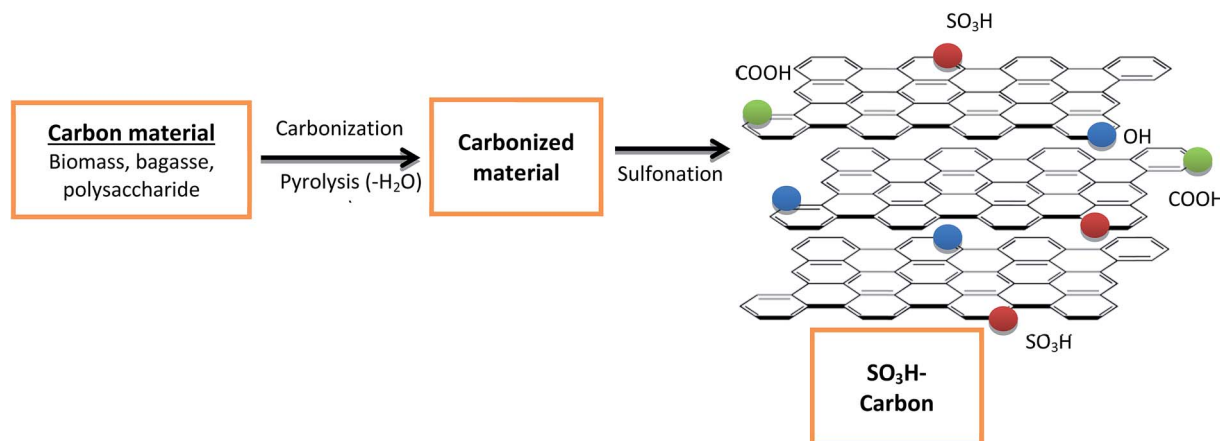


Fig. 12 Preparation of SO₃H-carbon.

consecutive batch runs), the conversion and selectivity results were not encouraging, that is 91% conversion and a 62% combined selectivity of DA and TA (slightly lower than those of other mentioned catalysts). Nevertheless, the density of Brønsted acid sites and mass transfer rate in the mesoporous channels of AC are the governing factors leading to TA synthesis.⁷⁵

A new class of sulfonated carbon catalysts termed “sugar catalyst” was recently reported. They were prepared *via* incomplete carbonization of simple carbohydrates (starch, cellulose, glucose, and sucrose) followed by sulphonation. Sánchez⁶¹ studied the effect of the porous system of a sulphonated sucrose-derived carbon prepared *via* silica-template carbonization for glycerol acetylation reaction. The presence of interconnected micro- and mesopores (45% in 0–2 nm micropores and 51% in 2–50 nm mesopores) in sucrose-derived carbon allowed effective surface sulfonation (C–SO₃H). High glycerol conversion (>99%) with high selectivity (50%) of TA was achieved during esterification (at 9 : 1 molar ratio of acetic acid to glycerol, 5 wt% catalyst, 180 °C optimum temperature, and 4 h reaction time).

Another study reported on the preparation of sulfonated carbon catalyst, which is derived from low-cost biomass (willow catkins), to be used in producing carbon support. The acid density of the sulphonated carbon is greatly influenced by sulphonation condition. The sulphonation temperature of 90 °C rendered the highest acidity of sulfonated carbon catalyst compared with that obtained at 100 °C, 80 °C, and 70 °C. Furthermore, the study indicated that ester selectivity is mainly correlated with catalyst acidity, where high acidity of sulfonated carbon yields 67.2% of DA and TA products. These types of catalysts showed good heat stability and high water tolerance at low production cost.⁷⁶

The acid-functionalized carbon was further improved using graphene oxide (GO) as carbon material. GO consists of oxygen-rich functional groups, such as SO₃H, carboxyl, hydroxyl, and epoxide groups, which provide moderate acidic site for glycerol esterification. The unique layered structure of graphene also improves the accessibility of reactant for adsorption during reaction. Moreover, the acid-functionalized GO enhanced the

acid density of the catalyst containing acidic SO₃H groups. The glycerol acetylation showed a good glycerol conversion of 98.5% with high selectivity of DA (60%) and TA (24.5%). In addition, GO has displayed high reusability without showing reduction in catalytic activity and changes in product distribution.⁷⁷

5.7 Others

A new type of catalyst, hydroxylated magnesium fluoride (MgF_{2-x}(OH)_x, where $x < 0.1$), which contains both Lewis and Brønsted acid sites, was synthesized for glycerol acetylation. The hydroxylated magnesium fluoride exhibits the following structural and chemical features: (i) high surface area with pore diameters at the mesopore range; (ii) very low solubility in strong polar solvents; (iii) hydrolysis resistance; (iv) medium-strength Lewis and Brønsted acid sites; (v) possibility of easy tuning of surface acidity; and (vi) nanoscopic particle dimension. MgF_{2-x}(OH)_x showed a majority of Lewis sites that are generated from Mg²⁺ sites of Mg–F bond, while Brønsted acid sites character from the Mg–OH group. The surface acidity of hydroxylated magnesium fluoride exhibiting high Lewis/Brønsted ratio sites is suggested to favor DA and TA formation during glycerol acetylation. Troncea³⁶ reported that the medium-strength Lewis acid sites of catalyst (such as incompletely coordinated Mg²⁺) exert a major effect on acetylation compared with Brønsted acid sites (M–OH groups) that favor MA formation. The increased selectivity to DA and TA with loading of Lewis sites may be explained by considering the double role of these sites: first, as active catalytic sites involved in the formation of the reactive electrophilic intermediate, and second, as dehydrating sites coordinating the water molecules formed during the reaction.

Recent studies have applied a magnetic solid acid catalyst (Fe–Sn–Ti(SO₄²⁻))-400 in glycerol acetylation and successfully produced 99% selectivity of TA with 100% total conversion.⁷⁸ All of the reactions were conducted at 80 °C, 2.5 wt% of catalyst, 5.6 mass ratio of acetic acid to glycerol, and 0.5 h reaction time. This magnetic-based catalyst consists of iron (Fe), tin (Sn), and titanium (Ti), sulfated by (NH₄)₂SO₄ solution, and calcined at

Table 5 Different kind of heterogeneous catalysts used for glycerol acetylation with acetic acid

Catalyst	Catalyst preparation	Catalyst characterization	Operating parameters	Performance	Ref.
Ion exchange resin catalyst Amberlyst 15	Commercial available	SSA = 37.6 m ² g ⁻¹ Acidity = 4.7 mmol g ⁻¹ PD = 30 nm <i>T</i> _{stability} = 120 °C PV = 0.4 cm ³ g ⁻¹ Moisture content = 48% Cross-linkage = 20% Acid strength, <i>H</i> ₀ = -3 to -2.2 <i>Amberlyst. 36:</i> SSA = 33 m ² g ⁻¹ Acidity = 5.4 mmol g ⁻¹	<i>T</i> = 110 °C <i>P</i> = 200 bar <i>t</i> = 2 h Molar ratio acetic acid to glycerol = 24 Flow rate of scCO ₂ = 1.2 mL min ⁻¹	<i>Y</i> = 41% <i>S</i> = 100% TA	41
(i) Amberlyst 36	Commercial available	Moisture content = 48% Cross-linkage = 20% Acid strength, <i>H</i> ₀ = -3 to -2.2 <i>Amberlyst. 36:</i> SSA = 33 m ² g ⁻¹ Acidity = 5.4 mmol g ⁻¹ PD = 24 nm <i>T</i> _{stability} = 140 °C PV = 0.2 cm ³ g ⁻¹ Moisture content = 52.4% Cross-linkage = 12% <i>Dowex 50Wx2:</i> Acidity = 4.8 mmol g ⁻¹ <i>T</i> _{stability} = 140 °C Moisture content = 76.7% Cross-linkage = 2% <i>Get-type</i> <i>Same as above</i>	<i>T</i> = 105 °C <i>t</i> = 10 h Molar ratio glycerol to acetic acid = 8 : 1	<i>Amberlyst 36:</i> <i>C</i> = 95.6% <i>S</i> = 70.3% MA; 4.5% DA <i>Dowex 50Wx2:</i> <i>C</i> = 95.2% <i>S</i> = 80.8% MA; 5.1% DA	42
(ii) Dowex 50Wx2		Moisture content = 76.7% Cross-linkage = 2% <i>Get-type</i> <i>Same as above</i>	<i>T</i> = 110 °C <i>t</i> = 270 min	<i>C</i> = 97.3% <i>S</i> = 47.7% DA; 44.5% TA	35
Amberlyst 15	Commercial available	Acidity: 2.1 mmol g ⁻¹ Acid strength, <i>H</i> ₀ = -5.6 to -3.0	Molar ratio acetic acid : glycerol = 9 : 1 <i>T</i> = 110 °C <i>t</i> = 3 h Catalyst loading = 0.15 g Molar ratio acetic acid : glycerol = 8 : 1	<i>C</i> = 98.4% <i>S</i> = 45% DA; 49.5% TA	44
Improved polymer-based solid acid catalyst (PES)	Precipitation and ion-exchange method The polymer with SSBBCBS and BCPS molar ratio of 5 : 5 (PES-50) was synthesized in ratio of: 0.05 mol of 4,4'-biphenol (BP), 0.025 mol of BCPS, 0.025 mol of SSBBCBS and 0.058 mol of K ₂ CO ₃ . The polymer PES-P was precipitated, followed by being washed thoroughly with hot deionized water for three times. The polymer was dried in oven at 100 °C for 12 h. As-synthesized PES-P polymer was exchanged in 0.5 M H ₂ SO ₄ at 25 °C for 6 h, and then filtrated				

Table 5 (Contd.)

Catalyst	Catalyst preparation	Catalyst characterization	Operating parameters	Performance	Ref.
Zeolite-based acid catalyst					
(i) Zeolite HZSM-5	Zeolites HZSM-5 and HUSY were purchased from Petrobras	HZSM-5: SSA = 374 m ² g ⁻¹ Acidity = 1.2 mmol g ⁻¹	T = 110 °C t = 30 min Molar ratio acetic acid : glycerol = 3 : 1	HZSM-5: C = 30% S = 10% DA & TA	48
(ii) Zeolite HUSY		T _{stability} = 386 °C Si/Al = 28 HUSY: SSA = 566 m ² g ⁻¹ Acidity = 1.9 mmol g ⁻¹ T _{stability} = 397 °C Si/Al = 2.6		HUSY: C = 14% S = 14% DA & TA	
PMo/NaUSY zeolite	<i>Preparation of NaUSY zeolite</i> HUSY zeolite was neutralized by 3 repeating 2 M NaCl at 80 °C. It was washed with distilled water and then dried at 120 °C	Acidity = 0.019 g _{HPA} g _{cat} ⁻¹ SSA = 713 m ² g ⁻¹ Micropore volume, mPV = 0.17 cm ³ g ⁻¹	T = not reported t = 3 h Catalyst = 10 wt% of glycerol	C = 68% S = 61% DA & TA	24
<i>Hydrothermal impregnation for PMo/NaUSY</i> The catalysts were prepared by hydrothermal impregnation method: by engaging molybdenum(vi)oxide on NaUSY, followed by neutralization and drying at 110 °C					
HPAs-based acid catalyst					
H ₄ SiW ₁₂ O ₄₀ /ZrO ₂	<i>Wetness impregnation method</i> HSiW/ZrO ₂ catalyst was prepared through incipient wetness impregnation method. Zirconia support was impregnated with 139 mmol/HSiW solution for 8 h, followed by drying (110 °C) and calcination (250 °C in static air, 4 h)	Acidity = 0.69 mmol g ⁻¹ SSA = 48.7 m ² g ⁻¹ PD = 10.7 nm	T = 120 °C t = 4 h Molar ratio acetic acid : glycerol = 10 : 1 Catalyst = 0.8 wt%	C = 100% S = 93.6% DA & TA	80
TPA/Cs ₂ -ZrO ₂	<i>Precipitation and impregnation method</i> Zirconia support was prepared by precipitation method and dried at 120 °C for 36 h. Zirconia support is then loaded by CsNO ₃ solution, calcined at 500 °C for 2 h Later, TPA supported Cs-zirconia was prepared by impregnation of 20 wt% of TPA solution, calcined at 350 °C for 4 h	PV = 0.17 cm ³ g ⁻¹ Acidity = not reported	T = 120 °C t = 4 h	C = 90% S = 55% DA; 5% TA	52
(i) TPA/MCM-41	<i>Impregnation method</i> Both TPA/MCM-41 and TPA/ZrO ₂ catalysts were prepared by incipient impregnation. MCM-41 was impregnated with 1% of TPA solution; while, ZrO ₂ with 10–40% of TPA, both dried at 100 °C for 10 h	TPA/MCM-41: SSA = 360 m ² g ⁻¹	Molar ratio acetic acid/glycerol = 1.5 Catalyst = 0.2 wt% T = 100 °C t = 360 min	TPA/MCM-41: C = 87%	53
(ii) TPA/ZrO ₂		Acidity = 0.855 mmol g ⁻¹ (majority of strong acid strength) TPA/ZrO ₂ : SSA = 146 m ² g ⁻¹ Acidity = 0.840 mmol g ⁻¹ (fully weak acid strength)	Mole ratio acetic acid : glycerol = 6 : 1 Catalyst = 0.15 g	S = 75% DA & TA	

Table 5 (Contd.)

Catalyst	Catalyst preparation	Catalyst characterization	Operating parameters	Performance	Ref.
HPW/Ag	<i>Ion-exchanged method</i> HPW/Ag was prepared by ion-exchanged method. A 0.1 mol L ⁻¹ AgNO ₃ solution was added drop-wise into HPW solution, aged 2 h, evaporated, dried at 80 °C (12 h) and calcined at 250 °C for 4 h	Acidity = 1.92 mequiv. g ⁻¹	T = 120 °C t = 4 h Molar ratio acetic acid : glycerol = 4 : 1 Catalyst = 10 wt% of glycerol Speed = 1200 rpm	C = 96.8% S = 90.7% DA & TA	54
TPA/Nb ₂ O ₅	<i>Impregnation method</i> TPA/Nb ₂ O ₅ was prepared by impregnation method. Nb ₂ O ₅ support was impregnated with 5–30 wt% of TPA in methanol, dried at 120 °C (12 h) and calcined in air at 300 °C for 2 h	Acidity = 1.149 mmol g ⁻¹ SSA = 66 m ² g ⁻¹ PV = 0.36 cm ³ g ⁻¹	T = 120 °C t = 4 h Molar ratio acetic acid : glycerol = 5 : 1 Catalyst = 4 wt% of glycerol	C = 90% S = 76% DA & TA	55
CsPWA (cesium phosphotungstate) catalyst	CsPWA was prepared in molar ratio Cs _{2.5} H _{0.5} PW ₁₂ O ₄₀ , by adding dropwise aqueous cesium carbonate (0.47 M) to H ₃ PW ₁₂ O ₄₀ (0.75 M) at room temperature. The precipitate was aged in aqueous mixture for 48 h at room temperature, dried in a rotary evaporator at 45 °C, then in an oven at 150 °C for 1.5 h	Acidity = 1.87 mmol g ⁻¹ SSA = 110 m ² g ⁻¹	T = 85 °C t = 120 min Molar ratio acetic acid : glycerol = 8 : 1 Catalyst = 7 wt%	C = 98.1% S = 75% DA & TA	2
Metal oxide-based acid catalyst SO ₄ ²⁻ /SnO ₂	<i>Wet-impregnation method</i> The catalyst was prepared by wet-impregnation method, where SnO ₂ was added into 0.5 M H ₂ SO ₄ solution (mass ratio of 10 wt% of SO ₄ ²⁻), dried at 120 °C (12 h) and calcined in air at 650 °C for 5 h	Acidity = 0.186 mmol g ⁻¹ SSA = 41 m ² g ⁻¹	T = 70 °C t = 2 h	C = 99%	56
SO ₄ ²⁻ /TiO ₂ -SiO ₂	<i>Precipitation and impregnation method</i> The catalyst was prepared by co-precipitation method, where Ti(OH) ₄ sol, Si(OC ₂ H ₅), C ₂ H ₅ OH and water were mixed to form Ti(OH) ₄ and Si(OH) ₄ mixture sol at 80 °C. It was then dried at 100 °C and calcined for 1 h at 500 °C TiO ₂ -SiO ₂ was sulfated with 1.0 M sulfuric acid for 1 h, dried under infrared lamp and calcined at 450 °C for 3 h	PD = 15.79 nm PV = 0.1623 cm ³ g ⁻¹ SSA = 550 m ² g ⁻¹	Molar ratio acetic acid : glycerol = 1 : 1 Catalyst = 5 wt% of glycerol Speed = 800 rpm Performed in solvent system T = 120 °C Catalyst = 5 wt% of glycerol	C = 91.4%	59
MoO ₃ /TiO ₂ -ZrO ₂	<i>Co-precipitation and impregnation method</i> MoO ₃ /TiO ₂ -ZrO ₂ was prepared by co-precipitation and impregnation method. The solids were dried at 120 °C (12 h) and calcined in air at 650 °C (5 h), where the ratio of TiO ₂ -ZrO ₂ is 1 to 1. Meanwhile, the ZrO ₂ was prepared in advance by precipitation of ZrOCl ₂ with drop-wise of NH ₄ OH solution	Acidity = 0.61 mmol g ⁻¹ SSA = 7 m ² g ⁻¹	Performed in solvent reaction system T = 120 °C t = 60 h Molar ratio acetic acid : glycerol = 6 : 1 Catalyst = 5 wt% of glycerol	C = 100% S = 80% DA & TA	25
SO ₄ ²⁻ /CeO ₂ -ZrO ₂	<i>Impregnation method</i> The catalyst was prepared by wet sulfonation-impregnation method, where 0.5 M H ₂ SO ₄ solution was mixed into 1 : 1 mol ratio of CeO ₂ -ZrO ₂ (based on oxides), stirred for 1 h, dried at 120 °C (3 h) and calcined for 5 h at 500 °C	SSA = 92 m ² g ⁻¹	T = 120 °C t = 1 h Molar ratio acetic acid : glycerol = 6 : 1 Catalyst = 5 wt%	C = 100% S = 74.2% DA & TA	60

Table 5 (Contd.)

Catalyst	Catalyst preparation	Catalyst characterization	Operating parameters	Performance	Ref.
Mesoporous silica-based acid catalyst MPA/SBA-15	<i>SBA-15 preparation</i> Pluronic P123 was dissolved in 1.8 M HCl, followed by addition of Brij S100. After 18 h, droplet of TEOS was added at 35–40 °C. The formed SBA-15 was dried at 90 °C (24 h), followed by DI water washing and re-dried at room temperature <i>Impregnation method</i> MPA/SBA-15 catalyst was impregnated by molybdophosphoric acid solution at room temperature for 24 h. It was dried and calcined in air for 6 h at 560 °C	Acidity = 0.86 mmol g ⁻¹ SSA = 754 m ² g ⁻¹ PD = 6.53 nm PV = 1.24 cm ³ g ⁻¹	T = 110 °C t = 3 h Molar ratio acetic acid : glycerol = 6 : 1 Catalyst = 2 wt% of glycerol	C = 100% S = 92.3% DA & TA	70
MP-nb-SBA-15	<i>nb-SBA-15 silica preparation:</i> Molar ratio of mixture was prepared at chemical ratio of: 1SiO ₂ : 0.005Pluronic P123 : 1.45HCl : 124H ₂ O. Ammonium niobate(v)oxalate was then added into mixture and stirred for 8 h at 55 °C. Thermal treating of solution was conducted at 80 °C without stirring for 16 h. The solid sample was filtered, washed and dried at 60 °C (12 h) and calcined at 550 °C (8 h) <i>Post synthesis of nb-SBA-15:</i> SBA-15 were heated (350 °C, 4 h) prior to addition of MPTMS in toluene solution. The mixtures were heated at 100 °C for 20 h, washed, dried at 100 °C (4 h). Oxidation of modifier was carried out by using H ₂ O ₂ and H ₂ SO ₄ solution <i>Hydrothermal method</i> The catalyst was prepared by dissolving of CTMABr in 0.4 Y% HCl (37%) solutions. Y(NO ₃) ₃ ·6H ₂ O was dropwise added to TEOS solution and then aged at 12 h (room temperature). It was washed, filtered, dried (12 h at 100 °C) and then calcined in air at 560 °C for 8 h (heating rate of 2 °C min ⁻¹) <i>Hydrothermal method</i> Both MCF support of the catalysts were prepared by dissolving of P123 into 0.7 M HCl solution, added by 1,3,5-trimethylbenzene, NH ₄ F, TEOS (after 1 h). Next, (i) ammonium niobate(v)oxalate hydrate; (ii) tantalum(v)ethoxide, was added to form Nb/MCF and Ta/MCF respectively. The solution was mixed (20 h), hydrothermal-treated (100 °C for 24 h), dried and calcined in air at 500 °C for 4 h	Acidity = 0.50 mequiv. g ⁻¹ SSA = 565 m ² g ⁻¹ PD = 6.8 nm (51%) PV = 0.38 cm ³ g ⁻¹	T = 150 °C t = 4 h Molar ratio acetic acid : glycerol = 9 : 1 Catalyst = 0.6 wt%	C = 94% S = 89% DA & TA S _{TA} = 40%	71
Y/SBA-3	<i>Hydrothermal method</i> The catalyst was prepared by dissolving of CTMABr in 0.4 Y% HCl (37%) solutions. Y(NO ₃) ₃ ·6H ₂ O was dropwise added to TEOS solution and then aged at 12 h (room temperature). It was washed, filtered, dried (12 h at 100 °C) and then calcined in air at 560 °C for 8 h (heating rate of 2 °C min ⁻¹) <i>Hydrothermal method</i> Both MCF support of the catalysts were prepared by dissolving of P123 into 0.7 M HCl solution, added by 1,3,5-trimethylbenzene, NH ₄ F, TEOS (after 1 h). Next, (i) ammonium niobate(v)oxalate hydrate; (ii) tantalum(v)ethoxide, was added to form Nb/MCF and Ta/MCF respectively. The solution was mixed (20 h), hydrothermal-treated (100 °C for 24 h), dried and calcined in air at 500 °C for 4 h	Acidity = 1.34 mmol g ⁻¹ SSA = 1568 m ² g ⁻¹ PD = 2.54 nm PV = 0.81 cm ³ g ⁻¹	T = 110 °C t = 2.5 h Molar ratio acetic acid : glycerol = 4 : 1 Catalyst = 5 wt% of glycerol Speed = 350 rpm T = 150 °C t = 4 h Molar ratio acetic acid : glycerol = 9 : 1 Catalyst = 4 wt% of glycerol	C = 100% S = 89% DA & TA	40
(i) Nb/MCF	<i>Hydrothermal method</i> Both MCF support of the catalysts were prepared by dissolving of P123 into 0.7 M HCl solution, added by 1,3,5-trimethylbenzene, NH ₄ F, TEOS (after 1 h). Next, (i) ammonium niobate(v)oxalate hydrate; (ii) tantalum(v)ethoxide, was added to form Nb/MCF and Ta/MCF respectively. The solution was mixed (20 h), hydrothermal-treated (100 °C for 24 h), dried and calcined in air at 500 °C for 4 h	Nb/MCF: Acidity = 0.32 mequiv. g ⁻¹ Ta/MCF: Acidity = 0.57 mequiv. g ⁻¹	Speed = 350 rpm T = 150 °C t = 4 h Molar ratio acetic acid : glycerol = 9 : 1 Catalyst = 4 wt% of glycerol	Nb/MCF: C = 89% S = 89% DA & TA Ta/MCF: C = 91% S = 87% DA & TA	72
(ii) Ta/MCF	<i>Hydrothermal method</i> Both MCF support of the catalysts were prepared by dissolving of P123 into 0.7 M HCl solution, added by 1,3,5-trimethylbenzene, NH ₄ F, TEOS (after 1 h). Next, (i) ammonium niobate(v)oxalate hydrate; (ii) tantalum(v)ethoxide, was added to form Nb/MCF and Ta/MCF respectively. The solution was mixed (20 h), hydrothermal-treated (100 °C for 24 h), dried and calcined in air at 500 °C for 4 h	Nb/MCF: Acidity = 0.32 mequiv. g ⁻¹ Ta/MCF: Acidity = 0.57 mequiv. g ⁻¹	Speed = 350 rpm T = 150 °C t = 4 h Molar ratio acetic acid : glycerol = 9 : 1 Catalyst = 4 wt% of glycerol	Nb/MCF: C = 89% S = 89% DA & TA Ta/MCF: C = 91% S = 87% DA & TA	72
Mesoporous carbon-based acid catalyst AC-SA5	<i>Hydrothermal method</i> The catalyst was prepared by hydrothermal method. Activated carbon was treated in 5 mol L ⁻¹ of H ₂ SO ₄ solution at 85 °C for 4 h	Blank AC SSA = 780 m ² g ⁻¹ PV = 0.52 cm ³ g ⁻¹ PSD = 500–710 μm AC-SA5 Acidity = 0.89 mmol g ⁻¹	T = 120 to 135 °C t = 3 h Molar ratio acetic acid : glycerol = 8 : 1 Catalyst = 4 wt% of glycerol	C = 91% S = 62% DA & TA	75

Table 5 (Contd.)

Catalyst	Catalyst preparation	Catalyst characterization	Operating parameters	Performance	Ref.
Sulfated silica template carbonized acid catalyst	<i>Hydrothermal method</i> Na ₂ SiO ₃ and H ₂ O were mixed at 70 °C to prepare silica template. Sucrose and HCl were then added into mixture. The solution was left for 24 h for polymerization. Carbonized of silica was conducted at 400 °C in N ₂ (5 h), followed by immerse with 3 M NaOH solution (12 h and 120 °C) and hot water washing Carbonized solids were left in contact overnight with fuming sulfuric acid (7% of SO ₃)	SSA = 742 m ² g ⁻¹ PV = 0.47 cm ³ g ⁻¹ PSD = 500–710 μm Mesopore SSA = 208 m ² g ⁻¹ Acidity = 1.35 mmol g ⁻¹ SSA = 556 m ² g ⁻¹ PD = 2–50 nm (51%) PV = 0.51 cm ³ g ⁻¹	T = 180 °C t = 4 h Molar ratio acetic acid : glycerol = 9 : 1 Catalyst = 5 wt%	C = 99.6% S = 50% TA	61
Sulfonated willow catkins-based carbon	<i>Hydrothermal method</i> The willow catkin (10 g) was carbonized in N ₂ at 450 °C for 5 h. The black powder (1 g) was then heated in 5 mL of concentrated H ₂ SO ₄ (95–98%) for 3 h at different temperatures. It was cooled down, filtered, dried at 80 °C (5 h). The dried powder (1 g) was then treated in 14 mL of fuming sulfuric acid (15 wt% SO ₃) at 100, 90, 80, and 70 °C, temperatures for 2 h and then cooled to room temperature <i>Hydrothermal and oxidation method</i>	Acidity = 5.14 mmol g ⁻¹ Content of -SO ₃ H = 2.85 mmol g ⁻¹	T = 120 °C t = 2 h Molar ratio acetic acid : glycerol = 5 : 1 Catalyst = 5 wt%	C = 98.4% S = 67.2% DA & TA	76
GO	Graphite (5 g) and NaNO ₃ (2.5 g) were placed into 115 mL H ₂ SO ₄ in an ice bath under vigorous stirring. After adding of 15 g KMnO ₄ , it was heated to 35 °C and stirred for extra 30 min. The mixture was diluted with water and re-heated to 98 °C. Subsequently, 50 mL H ₂ O ₂ (30 wt%) was added, followed by filtered, washed, dried (50 °C). Then, the dispersed GO was kept in water for sonication (1 h), centrifuged and dried at ambient temperature	Not reported	T = 120 °C t = 1 h Molar ratio acetic acid : glycerol = 10 : 1 Catalyst = 0.1 g	C = 98.5% S = 94.5% DA & TA S _{DA} = 60%	77
Others MgF _{2-x} (OH) _x , x < 0.1	<i>Hydrothermal method</i> Metallic Mg was dissolved in methanol (50 mL) at room temperature overnight. After heating under reflux conditions for 3 h, HF solution was added to the formed Mg(OCH ₃) ₂ solution, then aged for 12 h and dried under vacuum at room temperature. The solid product thus obtained was then further dried under vacuum at 70 °C for 5 h	Acidity = 0.33 mmol g ⁻¹ SSA = 424 m ² g ⁻¹ PV = 0.25 cm ³ g ⁻¹ PD = 2.2 nm	T = 100 °C t = 22 h Molar ratio acetic acid : glycerol = 3 : 1	C = >99% S = 85% DA & TA	36
Fe-Sn-Ti(SO ₄ ²⁻) ₄₀₀	<i>Precipitation and hydrothermal method</i> The magnetic matrix was made by mixture of [Fe ₂ SO ₄ /Fe ₂ (SO ₄) ₃] at 45 °C. The matrix (0.1 mol L ⁻¹) was then treated with stannic chloride pentahydrate (17.5 g), tetrabutyl titanate (10 mL) and NH ₃ ·H ₂ O. The formed solid sample is dried (100 °C) and further sulfated with (NH ₄) ₂ SO ₄ solution for 24 h, washed, filtered, dried and calcined at different temperatures	SSA = 18.88 m ² g ⁻¹ PV = 0.15 cm ³ g ⁻¹ PD = 3.8 nm	T = 80 °C t = 30 min Mass ratio acetic acid to glycerol = 5.6 Catalyst = 2.5 wt%	C = 100% S = 99% TA; 1% DA	78

SSA = specific surface area of catalyst; PD = pore diameter of a particle; PS = particle size of catalyst; PV = pore volume of catalyst; PSD = particle size distribution of catalyst. C = conversion, S = selectivity, Y = yield.

400 °C. The calcination temperature is a crucial factor to develop a good acid strength of the catalyst given that a catalyst calcined at 400 °C displays weak acid sites. The catalysts calcined at 500 °C, 600 °C, and 700 °C promoted the formation of a superacid structure. Furthermore, the acidity of magnetic catalyst is mainly contributed by Lewis acid (from Sn and Ti metal cations) and Brønsted acid (from proton of –OH groups). Both the Lewis and Brønsted acid sites play key role in activating the carbonyl group from acetic anhydride, which is further attacked by glycerol molecule for esterification process. The (Fe–Sn–Ti(SO₄²⁻))-400 catalyst exhibits good stability during catalyst recyclability test. Unfortunately, (Fe–Sn–Ti(SO₄²⁻))-400 demonstrated a water intolerance behavior as selectivity of TA is reduced to 26% when small amount of water was added during the reaction. This work also concluded that the catalytic activity is highly dependent on the acid strength but not on the total acid amount of the catalyst. Similar fact was also supported by Huang *et al.*,⁷⁹ where the presence of both Lewis and Brønsted acid sites are observed from sulfated Sr–Fe oxide and sulfated Ca–Fe oxide catalysts, respectively. The study summarized that Brønsted acid sites are able to catalyze the esterification of fatty acids *via* the protonation of the acid group (–COOH) to give oxonium ions, while the Lewis acid sites catalyze the esterification of fatty acids through the coordination of acid groups on the active sites. Table 5 shows the different types of heterogeneous catalysts used in glycerol acetylation using acetic acid.

6. Conclusions

Glycerol acetylation using acetic acid allows the cost-effective production of MA, DA, or TA compared with the use of acetic anhydride. Despite the spontaneous reaction and formation of electrophilic intermediates in catalytic acetylation of glycerol, the combined high conversion and selectivity of DA and TA can now be attained under mild reaction environment by using a well-designed heterogeneous acid catalyst. For TA, the magnetic solid acid catalyst (Fe–Sn–Ti(SO₄²⁻))-400 is currently the most competent catalyst because 99% selectivity of TA with a 100% total conversion was attained. However, TA formation is strongly affected by the acidity of the catalyst (more specifically by weak acid strength), by pore aperture (sufficient pore space to facilitate formation of large molecule), as well as by the correct shape–structure (high cross-linkage) at high molar ratio of acetic acid to glycerol (9 : 1). By contrast, low-pore catalyst should be used to generate high selectivity of small MA under excessive glycerol concentration (1 : 8 molar ratio of acetic acid to glycerol). The vital roles of the catalyst to increase product selectivity include controlling the acid sites, pore diameter, hydrolysis resistance, and hydrophobicity, whereas the molar ratio of acetic acid to glycerol is the more influential factor that improves the combined selectivity of DA and TA. Developing a hydrophobic-enhanced magnetic solid acid catalyst to overcome the problem on water deactivation and subsequently developing a scalable high-conversion-selectivity catalyst is strongly recommended.

Abbreviations

MA	Monoacetin
DA	Diacetin
TA	Triacetin
TBA	<i>tert</i> -Butyl alcohol
GMBE	Mono- <i>tert</i> butyl ether
GDDBE	Glycerol di- <i>tert</i> butyl ether
GTBE	Glycerol tertiary butyl ether
GEE	Glycerol ethyl ether
mono-GEE	Glycerol mono-ethyl ether
di-GEE	Glycerol di-ethyl ether
tri-GEE	Glycerol tri-ethyl ether
TBA	<i>tert</i> -Butyl alcohol
PES	Polymer-based acid
H ₃ PMO ₁₂ O ₄₀	Dodeca-molybdophosphoric acid
HPAS	Heteropolyacids
HSiW	Silicotungstic acid
HPW	Phosphotungstic acid
HPMo	Phosphomolybdic acid
TPA	12-Tungstophosphoric acid
SnO ₂	Tin oxide
MPTMS	3-Mercaptopropyl trimethoxysilane
MCF	Mesostructured cellular foams
AC	Activated carbon
GO	Graphene oxide

Acknowledgements

The authors thank University of Malaya for supporting this research under High Impact Research grant (Grant Number: UM.C/625/1/HIR/MOHE/ENG/59). The Laboratoire Génie Chimique of Campus INP-ENSIACET, SBUM scholarship and French government scholarship are gratefully acknowledged.

References

- 1 L. J. Konwar, P. Mäki-Arvela, P. Begum, N. Kumar, A. J. Thakur, J.-P. Mikkola, R. C. Deka and D. Deka, *J. Catal.*, 2015, **329**, 237–247.
- 2 S. Sandesh, P. Manjunathan, A. B. Halgeri and G. V. Shanbhag, *RSC Adv.*, 2015, **5**, 104354–104362.
- 3 Food and Agriculture Organization of the United Nations (OECD), *OECD-FAO Agricultural Outlook 2015*, OECD Publishing, Paris, 2015.
- 4 R. Ciriminna, C. d. Pina, M. Rossi and M. Pagliaro, *Eur. J. Lipid Sci. Technol.*, 2014, **116**, 1432–1439.
- 5 A. B. Leoneti, V. Aragão-Leoneti and S. V. W. B. de Oliveira, *Renewable Energy*, 2012, **45**, 138–145.
- 6 M. Ayoub and A. Z. Abdullah, *Renewable Sustainable Energy Rev.*, 2012, **16**, 2671–2686.
- 7 D. T. Johnson and K. A. Taconi, *Environ. Prog.*, 2007, **26**, 338–348.
- 8 M. O. Sonnati, S. Amigoni, E. P. Taffin de Givenchy, T. Darmanin, O. Choulet and F. Guitard, *Green Chem.*, 2013, **15**, 283–306.

- 9 B. Dou, C. Wang, Y. Song, H. Chen and Y. Xu, *Energy Convers. Manage.*, 2014, **78**, 253–259.
- 10 M. Pagliaro, R. Ciriminna, H. Kimura, M. Rossi and C. Della Pina, *Angew. Chem., Int. Ed.*, 2007, **46**, 4434–4440.
- 11 P. S. Kong, M. K. Aroua and W. M. A. W. Daud, *Renewable Sustainable Energy Rev.*, 2016, **63**, 533–555.
- 12 P. S. Kong, M. K. Aroua and W. M. A. W. Daud, *Rev. Chem. Eng.*, 2015, **31**, 437–451.
- 13 N. Rahmat, A. Z. Abdullah and A. R. Mohamed, *Renewable Sustainable Energy Rev.*, 2010, **14**, 987–1000.
- 14 B. A. Meireles, S. C. Pinto, V. L. P. Pereira and G. G. e. Leitao, *J. Sep. Sci.*, 2011, **34**, 971–977.
- 15 N. Viswanadham and S. K. Saxena, *Fuel*, 2013, **103**, 980–986.
- 16 J. A. Melero, G. Vicente, G. Morales, M. Paniagua, J. M. Moreno, R. Roldán, A. Ezquerro and C. Pérez, *Appl. Catal., A*, 2008, **346**, 44–51.
- 17 F. Frusteri, F. Arena, G. Bonura, C. Cannilla, L. Spadaro and O. Di Blasi, *Appl. Catal., A*, 2009, **367**, 77–83.
- 18 J. A. Melero, G. Vicente, M. Paniagua, G. Morales and P. Muñoz, *Bioresour. Technol.*, 2012, **103**, 142–151.
- 19 S. Pariente, N. Tanchoux and F. Fajula, *Green Chem.*, 2009, **11**, 1256–1261.
- 20 M. R. Anuar, A. Z. Abdullah and M. R. Othman, *Catal. Commun.*, 2013, **32**, 67–70.
- 21 P. Guerrero-Urbaneja, C. García-Sancho, R. Moreno-Tost, J. Mérida-Robles, J. Santamaría-González, A. Jiménez-López and P. Maireles-Torres, *Appl. Catal., A*, 2014, **470**, 199–207.
- 22 Croda, Priacetin™: Triacetin, <http://www.crodaindustrialchemicals.com/home.aspx?s=131&r=185&p=4833>, (accessed 25 Feb, 2014).
- 23 International Process Plants, Triacetin Plant, <http://www.ippe.com/plants/600496/triacetin.pdf>, (accessed 25 Feb, 2014).
- 24 P. Ferreira, I. M. Fonseca, A. M. Ramos, J. Vital and J. E. Castanheiro, *Catal. Commun.*, 2009, **10**, 481–484.
- 25 P. S. Reddy, P. Sudarsanam, G. Raju and B. M. Reddy, *Catal. Commun.*, 2010, **11**, 1224–1228.
- 26 TREATT, market report November 2011, http://www.getece.com/brochure/Treatt_Market_Report_November_2011.pdf, (accessed 25 Feb, 2014).
- 27 B. Katryniok, S. Paul, V. Bellière-Baca, P. Rey and F. Dumeignil, *Green Chem.*, 2010, **12**, 2079–2098.
- 28 M. Bloch, L. Bournay, D. Casanave, J. A. Chodorge, V. Coupard, G. Hillion and D. Lorne, *Oil Gas Sci. Technol.*, 2008, **63**, 405–417.
- 29 N. P. C. Services, Glycerol Triacetate (triacetin), <http://www.niir.org/profiles/profile/1895/glycerol-triacetate-triacetin.html>, (accessed 6 August, 2015).
- 30 E. Oleochemicals, Emery Oleochemicals starts work on Euro20mil expansion projects in Loxstedt, Germany, http://www.emeryoleo.com/individual_news.php?g=54, 29 June 2016.
- 31 C. J. Howell, W. D. R. Mc and T. L. Steiner, European patent, EP 0244208, 1991.
- 32 R. I. C. Ltd., Glycerin Triacetate (Triacetin), <http://docslide.us/documents/glycerin-triacetatetriacetin-food-grade.html>, (accessed 5 August, 2015).
- 33 J. I. García, H. García-Marín and E. Pires, *Green Chem.*, 2014, **16**, 1007–1033.
- 34 A. Zięba, A. Drelinkiewicz, P. Chmielarz, L. Matachowski and J. Stejskal, *Appl. Catal., A*, 2010, **387**, 13–25.
- 35 L. Zhou, E. Al-Zaini and A. A. Adesina, *Fuel*, 2013, **103**, 617–625.
- 36 S. B. Troncea, S. Wuttke, E. Kemnitz, S. M. Coman and V. I. Parvulescu, *Appl. Catal., B*, 2011, **107**, 260–267.
- 37 S. Yan, S. O. Salley and K. S. Ng, *Appl. Catal., A*, 2009, **353**, 203–212.
- 38 E. Gürbüz, J. Q. Bond, J. A. Dumesic and Y. Román-Leshkov, in *The Role of Catalysis for the Sustainable Production of Bio-fuels and Bio-chemicals*, ed. K. S. T. A. L. Stöcker, Elsevier, Amsterdam, 2013, pp. 261–288, DOI: 10.1016/b978-0-444-56330-9.00008-5.
- 39 A. Zięba, A. Drelinkiewicz, P. Chmielarz, L. Matachowski and J. Stejskal, *Appl. Catal., A*, 2010, **387**, 13–25.
- 40 M. S. Khayoon, S. Triwahyono, B. H. Hameed and A. A. Jalil, *Chem. Eng. J.*, 2014, **243**, 473–484.
- 41 M. Rezayat and H. S. Ghaziaskar, *Green Chem.*, 2009, **11**, 710–715.
- 42 I. Dosuna-Rodríguez and E. M. Gaigneaux, *Catal. Today*, 2012, **195**, 14–21.
- 43 A. Ignatyev Igor, V. Doorslaer Charlie, G. N. Mertens Pascal, K. Binnemans and E. d. Vos Dirk, *Holzforchung*, 2012, **66**, 417.
- 44 Z.-Q. Wang, Z. Zhang, W.-J. Yu, L.-D. Li, M.-H. Zhang and Z.-B. Zhang, *Fuel Process. Technol.*, 2016, **142**, 228–234.
- 45 C. X. da Silva, V. L. Gonçalves and C. J. Mota, *Green Chem.*, 2009, **11**, 38–41.
- 46 S. Shaikhutdinov and H.-J. Freund, *ChemPhysChem*, 2013, **14**, 71–77.
- 47 A. Galadima and O. Muraza, *Microporous Mesoporous Mater.*, 2015, **213**, 169–180.
- 48 V. L. C. Gonçalves, B. P. Pinto, J. C. Silva and C. J. A. Mota, *Catal. Today*, 2008, **133–135**, 673–677.
- 49 T. Okuhara, *Chem. Rev.*, 2002, **102**, 3641–3666.
- 50 I. V. Kozhevnikov, *Chem. Rev.*, 1998, **98**, 171–198.
- 51 S. Zhu, Y. Zhu, X. Gao, T. Mo, Y. Zhu and Y. Li, *Bioresour. Technol.*, 2013, **130**, 45–51.
- 52 K. Jagadeeswaraiyah, M. Balaraju, P. S. S. Prasad and N. Lingaiah, *Appl. Catal., A*, 2010, **386**, 166–170.
- 53 A. Patel and S. Singh, *Fuel*, 2014, **118**, 358–364.
- 54 S. Zhu, X. Gao, F. Dong, Y. Zhu, H. Zheng and Y. Li, *J. Catal.*, 2013, **306**, 155–163.
- 55 M. Balaraju, P. Nikhitha, K. Jagadeeswaraiyah, K. Srilatha, P. S. Sai Prasad and N. Lingaiah, *Fuel Process. Technol.*, 2010, **91**, 249–253.
- 56 B. Malleshm, P. Sudarsanam and B. M. Reddy, *Catal. Sci. Technol.*, 2013, **4**, 803–813.
- 57 M. Kim, S. O. Salley and K. Y. S. Ng, *US Pat.*, US20120283459 A1, 2012.
- 58 M. Borges and L. Díaz, *Renewable Sustainable Energy Rev.*, 2012, **16**, 2839–2849.

- 59 H. Yang, R. Lu, J. Zhao, X. Yang, L. Shen and Z. Wang, *Mater. Chem. Phys.*, 2003, **80**, 68–72.
- 60 P. S. Reddy, P. Sudarsanam, G. Raju and B. M. Reddy, *J. Ind. Eng. Chem.*, 2012, **18**, 648–654.
- 61 J. A. Sánchez, D. L. Hernández, J. A. Moreno, F. Mondragón and J. J. Fernández, *Appl. Catal., A*, 2011, **405**, 55–60.
- 62 Z. Hasan, J. W. Yoon and S. H. Jhung, *Chem. Eng. J.*, 2015, **278**, 105–112.
- 63 G. M. Ziarani, N. Lashgari and A. Badieli, *J. Mol. Catal. A: Chem.*, 2015, **397**, 166–191.
- 64 S. Miao and B. H. Shanks, *J. Catal.*, 2011, **279**, 136–143.
- 65 J. n. Pérez-Pariente, I. Díaz, F. Mohino and E. Sastre, *Appl. Catal., A*, 2003, **254**, 173–188.
- 66 C. Márquez-Alvarez, E. Sastre and J. Pérez-Pariente, *Top. Catal.*, 2004, **27**, 105–117.
- 67 A. Galarneau, H. Cambon, F. Di Renzo, R. Ryoo, M. Choi and F. Fajulaa, *New J. Chem.*, 2003, **27**, 73–79.
- 68 B. S. Kumar, A. Dhakshinamoorthy and K. Pitchumani, *Catal. Sci. Technol.*, 2014, **4**, 2378–2396.
- 69 U. Flessner, D. J. Jones, J. Rozière, J. Zajac, L. Storaro, M. Lenarda, M. Pavan, A. Jiménez-López, E. Rodríguez-Castellón, M. Trombetta and G. Busca, *J. Mol. Catal. A: Chem.*, 2001, **168**, 247–256.
- 70 M. S. Khayoon and B. H. Hameed, *Appl. Catal., A*, 2012, **433–434**, 152–161.
- 71 M. Trejda, K. Stawicka, A. Dubinska and M. Ziolk, *Catal. Today*, 2012, **187**, 129–134.
- 72 K. Stawicka, M. Trejda and M. Ziolk, *Appl. Catal., A*, 2013, **467**, 325–334.
- 73 L. J. Konwar, J. Boro and D. Deka, *Renewable Sustainable Energy Rev.*, 2014, **29**, 546–564.
- 74 M. Okamura, A. Takagaki, M. Toda, J. N. Kondo, K. Domen, T. Tatsumi, M. Hara and S. Hayashi, *Chem. Mater.*, 2006, **18**, 3039–3045.
- 75 M. S. Khayoon and B. H. Hameed, *Bioresour. Technol.*, 2011, **102**, 9229–9235.
- 76 M.-L. Tao, H.-Y. Guan, X.-H. Wang, Y.-C. Liu and R.-F. Louh, *Fuel Process. Technol.*, 2015, **138**, 355–360.
- 77 X. Gao, S. Zhu and Y. Li, *Catal. Commun.*, 2015, **62**, 48–51.
- 78 J. Sun, X. Tong, L. Yu and J. Wan, *Catal. Today*, 2016, **264**, 115–122.
- 79 C.-C. Huang, C.-J. Yang, P.-J. Gao, N.-C. Wang, C.-L. Chen and J.-S. Chang, *Green Chem.*, 2015, **17**, 3609–3620.
- 80 S. Zhu, Y. Zhu, X. Gao, T. Mo, Y. Zhu and Y. Li, *Bioresour. Technol.*, 2013, **130**, 45–51.